Resonance Excitation and Electron Capture By Low Charged Ions

by

Abdulrahman Abdulaziz Al-Mulhem

A Thesis Presented to the

FACULTY OF THE COLLEGE OF GRADUATE STUDIES

KING FAHD UNIVERSITY OF PETROLEUM & MINERALS

DHAHRAN, SAUDI ARABIA

In Partial Fulfillment of the
Requirements for the Degree of

MASTER OF SCIENCE

In

PHYSICS

April, 1992

Order Number 1354111

Resonance excitation and electron capture by low charged ions

Al-Mulhem, Abdulrahman Abdulaziz, M.S.

King Fahd University of Petroleum and Minerals (Saudi Arabia), 1992

U·M·I

300 N. Zeeb Rd.
Ann Arbor, MI 48106

RESONANCE EXCITATION AND ELECTRON CAPTURE BY LOW CHARGED IONS

by

Abdulrahman Abdulaziz Al-Mulhem

A Thesis Presented to the
FACULTY OF COLLEGE OF GRADUATE STUDIES

In Partial Fulfillment of the Requirements
for the degree

MASTER OF SCIENCE

IN

PHYSICS

KING FAHD UNIVERSITY OF PETROLEUM AND MINERALS

Dhahran, Saudi Arabia

APRIL 1992

KING FAND UNIVERSITY OF PETROLEUM AND MINERALS
DHAHRAN 31261, SAUDI ARABIA

COLLEGE OF GRADUATE STUDIES

This thesis, written by Abdulrahman Abdulaziz Al-Mulhem under the direction of his Thesis Advisor and approved by his Thesis Committee, has been presented to and accepted by the Dean of the College of Graduate Studies, in partial fulfillment of the requirements for the degree of MASTER OF SCIENCE.

Thesis Committee

I. Nasser
Chairman: Associate Professor I. Nasser

Riazuddin
Member : Professor Riazuddin

Harry G. Mavromatis
Member : Professor H. Mavromatis

O. B. Dabbousi
Member : Professor O. Dabbousi

Department Chairman

Dean, College of Graduate Studies

Date

To the memory of my brother

Air Lieutenant

Abdulhameed Abdulaziz Al-Mulhem

Acknowledgement

I would like to express my deep appreciation to my thesis advisor, Dr. Ibraheem Nasser, for suggesting the topic of this thesis and for his continuous encouragement, guidance and patience which made the completion of this work possible. My debit to him is beyond measure.

I would also like to express my sincere thanks to the members of my thesis committee, Professors: Riazuddin, Harry Mavromatis, and Osama Dabbousi for reviewing the manuscript and the thoughtful comments and criticisms.

I would like to express my acknowledgement to my colleagues, friends, and cousins for their constant encouragement and advice which gave me added incentive to complete this work.

I appreciate the assistance of King Fahd University of Petroleum and Minerals Data Processing Center, whose facilities were used extensively in carrying out the calculations required to complete the study.

I am grateful to my parents for their love, patience, guidance, and prayers from my early school years to this time. I shall ever be grateful to them.

Finally, I would like to express my thanks to my dear wife Baheya for her patience and sacrifice which have been major factors in the completion of this research.

TABLE OF CONTENTS

Page

LIST OF TABLES

LIST OF FIGURES

THESIS ABSTRACT

NAME: ABDULRAHMAN ABDULAZIZ AL-MULHEM

TITLE: RESONANCE EXCITATION AND ELECTRON CAPTURE BY LOW CHARGED IONS

FIELD: PHYSICS

DATE: APRIL 1992

We calculated the dielectronic recombination and resonance excitation cross sections and rate coefficients of Al-like S^{3+} ion at low energies ($e_c < 1.22$ Ry) for the process in which the 3s electron of the ground state $(3s^2\ 3p)^2P$ is excited to the 3p level of the first excited state $(3s\ 3p^2)$ and the continuum electron is captured to high Rydberg state (n ℓ). We included the contributions from the multiplets of the first excited state namely ^4P, ^2D, ^2S, and ^2P. Single configuration and nonrelativistic Hartree-Fock wave functions in LS coupling were employed in the evaluation of the probability amplitudes required in the calculation of the cross sections and rate coefficients. We used energy bin of width $\Delta e_c = 0.01$ Ry in averaging the cross sections and rate coefficients.

MASTER OF SCIENCE DEGREE

KING FAHD UNIVERSITY OF PETROLEUM AND MINERALS
Dhahran, Saudi Arabia

APRIL 1992

خلاصة الرساله

الإسم :عبد الرحمن بن عبد العزيز بن عبد الله الملحم

عنوان الرساله : التهيج الرنيني و اصطياد الالكترون بواسطة الايونات المنخفضة الشحنة

التخصص : فيزياء

تاريخ الشهادة : شوال ١٤١٢

قمنا بحساب المقاطع المستعرضة لإعادة الربط الثناءي الإلكتروني و التهيج الرنيني لايون الكبريت الرابع شبيه الالمنيوم عند طاقات منخفضة للالكترون الساقط للعمليه الناتجه عن انتقال الكترون مستوي الطاقه الارضي الي المستوي المستثار الاول و اصطياد الالكترون الساقط في مستوي الطاقه من نوع رايدبرغ العالي. اخذنا بعين الاعتبار الانتقالات الناتجة عن انقسامات مستوي الطاقه الاول بسبب تداخل كمية الحركة الزاوية بكمية الحركة الذاتية. استخدمنا في حساباتنا الاقتران الزاوي المغزلي، و في تقييم الاحتمالات المطلوبه لحساب المقاطع المستعرضه و معاملات التغير استخدمنا دوال موجيه غير نسبيه من نوع هارتري-فوك. إستخدمنا فرق طاقه قدره ٠.٠١ رايدبرغ في حساب المتوسط الحسابي للمقاطع المستعرضه و معاملات التغير.

درجة الماجستير في العلوم

جامعة الملك فهد للبترول و المعادن
الظهران، المملكة العربية السعودية

شوال ١٤١٢

CHAPTER 1

INTRODUCTION

The process of dielectronic recombination (DR) starts with the collision of a projectile electron (continuum electron) with a positively charged target ion (i). A bound electron in i may be excited to an upper ionic level, while the projectile electron may be captured into a highly excited state of the ionic target. As a result, a doubly excited state (d) is formed. This intermediate state is stabilized either by emission of radiation or by Auger emission of an electron. If radiation emission occurs, then a singly excited ion appears in the final state and the DR process is complete. If, instead, electron emission occurs, then resonance excitation (RE) is the result.

The two processes, i. e. DR and RE are formulated as follows

$$e + (A^{z+} = i) \rightarrow ((A^{(z-1)+})^{**} = d) \rightarrow ((A^{(z-1)+})^{*} = f) + \gamma \qquad \text{DR} \quad (1.1)$$

$$\rightarrow ((A^{z+})^{*} = i') + e' \qquad \text{RE} \quad (1.2)$$

It is now well established that the DR process plays a very important role in the rapid radiative cooling of high-temperature astrophysical and laboratory plasmas. Therefore, accurate determination of DR cross sections and rate coefficients for many different ions is necessary for precise determination of the characteristic and behavior of such types of plasmas. Accurate calculations of the DR rate coefficients are, however, lengthy and tedious due to the multistep nature of the process of free electron capture into one of a doubly infinite set of intermediate resonance states. These states may then decay either by Auger electron emission of by radiative decay to final state, which could itself be unstable with respect to further Auger emission. Due to these complications theoretical calculation requires numerous drastic approximations and preciseness of calculations depends on where the results are going to be used. Consequently only a limited number of ions have been treated theoretically and experimentally and various semi-empirical formulas are employed for practical applications.

The process of DR goes back in history to 1942 when Massey and Bates[1] first described it, and since then much effort has been made both theoretically and experimentally to understand the various aspects of DR. However, it was not until 1964 when Burgess[2] first formulated it in a semi-

empirical fashion and found that DR process is more important at high temperatures than has been previously thought by Massey and Bates[1].

Before 1964 the dielectronic recombination process was not included in the ionization-recombination theory of the solar corona and coronal temperatures deduced from the theory of ionization equilibrium implied that either the ionization rates were too large or the recombination rates were too small. Burgess[2] in 1964 pointed out that this argument is not valid at high temperatures at which point a complete Rydberg series of autoionizing resonances must be considered. He then made the assumption that the total dielectronic recombination rate is dominated by a subset of dipole transition for a typical set of coronal ions. The resulting rate coefficients were found to be two to three orders of magnitude larger than the rate coefficients for the direct radiative process.

Because of various technical difficulties, experimental study of DR cross sections was not possible until recently, and most of the available information on DR has been obtained theoretically (Hahn[3]).

The experimental situation has changed during the past few years, and at present there are available several direct

measurements of the coefficient α^{DR}, and the dielectronic recombination cross section σ^{DR}. However, no experimental attempt has been made to measure the cross sections and rate coefficients of S IV ion.

During the past few years, several theoretical calculations have been made to understand the various perturbations on DR cross sections and rate coefficients for ions belonging to several isoelectronic sequences.

The experimental and theoretical work showed that DR is a very efficient recombination mechanism which not only influences the ionization balance but also cools solar corona and laboratory plasmas. Hence, DR has been the subject of intense theoretical and experimental work in the atomic collision research. Several theoretical groups have been trying to improve the existing semiemperical formulae for the DR rate coefficients for all isoelectronic sequences. In addition, some low-Z isoelectronic sequences such as C-like and N-like ions have not been studied to date because of their complicated coupling structure. Therefore, much work on DR is still needed in the future, in parallel to the current research on the other atomic collision processes.

In this work we are motivated to calculate the DR cross sections and rate coefficients of Al-like S^{3+} ion as part of a

series we intend to cover in order to test the theoretical approach employed.

In section 1.1, we review[4,5,6,7] the theoretical method used in the present work.

In chapter 2, we attempt to calculate the resonant electron capture and elastic scattering cross sections and rate coefficients of the ground state $(3s^2\ 3p)^2P$ of Al-like P^{2+} and S^{3+} ions at low energies. We are going to evaluate Auger and radiative transition probabilities for low n ($n < 11$), and extrapolate them to high n-values. Single configuration non-relativistic Hartree-Fock wavefunctions in LS coupling are used to evaluate these probabilities.

In chapter 3, we use the same method of calculation of chapter 2 to calculate DR cross sections and rate coefficients of S^{3+} for the process in which the 3s electron is excited to the 3p state and the projectile electron is captured to high Rydberg state. The transitions from the ground state $(3s^2\ 3p)^2P$ and the multiplets of the first excited state $(3s\ 3p^2)$ will be considered explicitly.

In chapter 4, we complete what was started in chapter 2 to calculate the resonance excitation and resonance elastic scattering cross sections and rate coefficients to cover not

only the first multiplet of the first excited state but all the multiplets.

1.1 THEORY OF DIELECTRONIC RECOMBINATION AND RESONANCE EXCITATION

DR and RE processes are examples of higher order processes in which an initial state (i) is passed to final state (f) through an intermediate state (d).

DR process takes place in low-density hot astrophysical and laboratory plasmas when electrons collide with ions. It proceeds in two steps: first continuum electrons undergo radiationless capture to form a (d) state and second the stabilization of the (d) state by emission of radiation.

RE process, on the other hand, has the same first step as in DR, but the (d) state is stabilized by the emission of an Auger electron.

The principal quantities that describe the DR and RE processes are the radiative transition probability A_a and Auger emission probability A_r, respectively.

Auger emission process was first observed by Auger in

1925, in which an inner shell vacancy is filled by one of the outer shell electrons.

The Auger emission probability is given by,

$$A_a = \frac{(2\pi)^2}{h} | \langle i| \frac{e^2}{r_{12}} |d\rangle |^2 \qquad (1.3)$$

The conservation of parity requires that both states on both sides of the operator V_{12} have the same parity. The unit of Auger rate is $(\text{time})^{-1}$. If we use Hartree as the unit of energy (1 Hartree = e^2/a_0 = 27.2 eV) and use Bohr radius a_0 as the unit of distance, then equation (1.3) becomes,

$$A_a = \frac{(2\pi)^2 e^2}{h\, a_0} | \langle i| \frac{1}{r_{12}} |d\rangle |^2 = \frac{2\pi}{\tau_0} | \langle i| \frac{1}{r_{12}} |d\rangle |^2 \qquad (1.4)$$

where $\tau_0 = 2.42 \times 10^{-17}$ sec is the atomic unit of time.

In the matrix element, the electron-electron operator is given by,

$$\hat{V}_{12} = \frac{1}{r_{12}} = \frac{1}{| r_1 - r_2 |} = \sum_{k=0}^{\infty} \frac{r_<^k}{r_>^{k+1}} P_k(\cos\omega) \qquad (1.5)$$

where $r_>(r_<)$ is the larger (smaller) of r_1 and r_2, ω is the angle between r_1 and r_2 and $P_k(\cos\omega)$ is a Legendre polynomial

given by[8],

$$P_k(\cos\omega) = \frac{4\pi}{2l+1} \sum_{m=-k}^{k} Y^*_{km}(\theta_1,\varphi_1)\, Y_{km}(\theta_2,\varphi_2) \qquad (1.6)$$

where Y_{km} are spherical harmonics.

The matrix element in (1.4) may be written in a convenient form as,

$$\langle il\, \hat{V}_{12}\, ld\rangle = \langle t,cl\, \hat{V}_{12}\, la,b\rangle \qquad (1.7)$$

where t denotes the wave function for the bound electron in the initial state (i), c denotes the continuum electron wave function and a and b denote the states in the intermediate state (d). The wave functions for t, a, and d are calculated in the non-relativistic single-configuration Hartree-Fock approximation and each wave function is assumed to be separable,

$$\psi_{nlm\alpha} = R_{nl}(r)\, Y_{lm}(\theta,\varphi)\, \chi_\alpha(\sigma) \qquad (1.8)$$

where $R_{nl}(r)$, $Y_{lm}(\theta,\varphi)$ and $x_a(\sigma)$ are the radial, angular and spin wave functions, respectively. The continuum wave function is calculated in the destorted wave approximation, its radial part behaves asymptotically ($r\to\infty$) as,

$$R_{k_c l_c}(r) \rightarrow \left(\frac{2}{\pi p_c}\right)^{1/2} \frac{1}{r} \sin\left[p_c r + \frac{Z_1}{p_c} \ln(2p_c r) - l_c \frac{\pi}{2} + \sigma_{l_c} + \delta_{l_c}\right] \qquad (1.9)$$

where p_c is the momentum of the continuum electron, σ_{l_c} is the Coulomb phase shift given by $\sigma_{l_c} = \arg \Gamma(l_c + 1 + \frac{i}{k_c})$ and δ_{l_c} is the phase shift due to Hartree-Fock potential of the core ion.

In the dipole approximation, the radiative transition between the states $d \equiv n_d, l_d, m$ and $f \equiv n_f, l_f, m'$ are possible only if the orbital and magnetic quantum numbers l, m change by[8],

$$\Delta l = l_f - l_d = \pm 1 \qquad (1.10)$$

$$\Delta m = m' - m = 0, \pm 1 \qquad (1.11)$$

and the parity of the two states is different, i.e.,

$$\text{even state} \leftrightarrow \text{odd state}$$

which are called the dipole selection rules. There are no limitations on the principal quantum numbers n_d and n_f. If $\Delta n = n_d - n_f = 0$, we refer to this transition as the $\Delta n = 0$ transition; otherwise it is the $\Delta n \neq 0$ transition. If the

conditions (1.10) and (1.11) are not fulfilled, then the dipole radiation is forbidden, in this case, quadrupole or magnetic radiation may be possible. The probability of such transition , however, is approximately $10^3 \sim 10^5$ times smaller than that for dipole transition. The radiative rate for single-electron transition, in the dipole approximation, from an intermediate state (d) to a final state (f) is given by,

$$A_r^{(0)}(d \rightarrow f) = \frac{(2\pi)^2}{h} | \langle f| \hat{D} |d\rangle |^2 \rho_f \qquad (1.12)$$

where the photon-electron interaction operator $\hat{D}$ is given by

$$\hat{D} = - (h\omega_{fd})^{1/2} (\vec{\epsilon} . \vec{r}) \qquad (1.13)$$

and the final density of states (ρ_f) is given by

$$\rho_f = (h)^{-3} (\frac{h^2\omega^2}{4\pi^2c^3}) \qquad (1.14)$$

Each resonance intermediate state (d) may decay by either radiative or electron emission; that is, it has Auger width $\Gamma_a(d)$ and radiative width $\Gamma_r(d)$. By adding these two widths, one will get the total resonance width of this state (d). This yields important information on the state (d) which is related to its life time. This is true not only in electron-ion

collisions but also in all other types of atomic collisions in which resonance intermediate states are involved. We have

$$\Gamma_a(d) = \sum_{l_c} A_a(d \rightarrow i, l_c) + \sum_{l'_c} A_a(d \rightarrow i', l'_c) \qquad (1.15)$$

where l_c takes on all allowed orbital angular momentum values for the continuum electron that conserve the parity between the initial ground state and the intermediate state, and l'_c for the orbital angular momentum of the Auger emitted electron corresponding to the singly-excited state (i'). Further,

$$\Gamma_r(d) = \sum_{f} A_r(d \rightarrow f) \qquad (1.16)$$

where f denotes all the allowed final states reached by radiative transitions. The total resonance width of the intermediate state is then defined as

$$\Gamma(d) = \Gamma_d(d) + \Gamma_r(d) \qquad (1.17)$$

The resonance width is related to the theoretical life time of a (d) state through the uncertainty principle which has the following general form

$$\Delta E \,.\, \Delta t \geq h \qquad (1.18)$$

where $\Delta E \equiv \Gamma(d)$ and $\Delta t \equiv \tau$.

The radiationless excitation-capture probability may be defined as

$$A_a = \frac{(2\pi)^2}{h} | \langle i | \frac{e^2}{r_{12}} | d \rangle |^2 \qquad (1.19)$$

which is related to the Auger rate for the time-reversed transition from the intermediate to the initial state by detailed balance

$$g_e \, g_i \, V_a(l_c, i \rightarrow d) = g_d \, A_a(d \rightarrow i, l_c) \qquad (1.20)$$

where g_i and g_d are the statistical weights of the initial and intermediate states, respectively, and $g_e = 2$ is the statistical factor for the spin of the continuum electron. Note that V_a is not related to the total Auger width $\Gamma_a(d)$, but related to the Auger rate for the initial state only.

For the DR process, it is convenient to define the radiative branching ratio as fluorescence yield, w(d). This is given by

$$\omega(d) = \frac{\Gamma_r(d)}{\Gamma_a(d) + \Gamma_r(d)} = \frac{\sum_f A_r(d \rightarrow f)}{\Gamma(d)} \qquad (1.21)$$

On the other hand, the branching ratio for the RE process may be called Auger yield because an Auger electron is emitted to proceed to the final state (i'), thus

$$Z(d) = \frac{\sum_{l'_c} A_a(d \rightarrow i', l'_c)}{\Gamma_a(d) + \Gamma_r(d)} \qquad (1.22)$$

Since the total Auger rate to the ground state (i) is always smaller than the total Auger rate to the singly excited state or states (i'), i.e.,

$$\sum_{l_c} A_a(d \rightarrow i, l_c) < \sum_{l'_c} A_a(d \rightarrow i', l'_c) \qquad (1.23)$$

hence the branching ratio B(d) for the decay of the doubly excited intermediate state (d) to the ground state (i)

$$B(d) = \frac{\sum_{l_c} A_a(d \rightarrow i, l_c)}{\Gamma_a(d) + \Gamma_r(d)} \qquad (1.24)$$

is sizable for the states (d) when only DR can take place (and not RE), but is very small when RE and DR compete strongly.

The differential cross section is defined in general as

$$d\sigma_{fi} = \frac{W_{fi}}{F_i} \tag{1.25}$$

where W_{fi} is the transition probability form an initial state (i) to a final state (d), and F_i is the initial state flux.

$$F_i = V_c = \frac{p_c}{m_c} \tag{1.26}$$

where v_c, p_c, and m_e are the incoming electron velocity, momentum, and mass, respectively. According to Fermi's Golden Rule, W_{fi} is given by

$$W_{fi} = \frac{(2\pi)^2}{h} | T_{fi}^{DR} |^2 \rho_f \tag{1.27}$$

Since DR proceeds from (i) to (f) through (d), the transition amplitude $T^{DR}_{i\to d\to f}$ carries information not only about (i) and (f) states but also about (d) state, we can write

$$T^{DR}_{i\to d\to f} = \sum_d \langle f|\hat{D}|d\rangle \, G_d^{\Gamma} \, \langle d|\hat{V}_{12}|i\rangle \tag{1.28}$$

where

$$G_d^{\Gamma} = \frac{1}{E_i - E_d + \frac{i\Gamma(d)}{2}} \tag{1.29}$$

with $E_i = e_i + e_c$, and e_c, e_i and E_d are the energies of the continuum electron, initial and intermediate states respectively, and $\Gamma(d)$ is the resonance width of the intermediate state, now we get

$$W_{fi} = \frac{(2\pi)^2}{h} \sum_d \frac{|\langle f|\widehat{D}|d\rangle|^2}{\Gamma(d)} \frac{2\pi\Gamma(d)}{(E_i - E_d)^2 + \Gamma^2(d)/4} 2\pi\, |\langle d|\widehat{V}_{12}|i\rangle|^2\, \rho_f \tag{1.30}$$

In the sharp resonance limit, we have

$$\mathrm{Lim}_{\Gamma(d)\to 0} \frac{\Gamma(d)/2\pi}{(E_i - E_d)^2 + \Gamma^2/4} = \delta(E_i - E_d) = \delta(e_c) \tag{1.31}$$

with the property that,

$$\int_{-\infty}^{+\infty} \delta(e_c)\, de_c = 1 \tag{1.32}$$

where the resonance condition requires $E_i = E_d$. Using equations (1.30) and (1.31) in (1.25) we get,

$$d\sigma^{DR}_{f\to d\to i} = \sum_d \frac{(2\pi)^2}{h} \frac{|\langle f|\widehat{D}|d\rangle|^2}{\Gamma(d)} \rho_f\, \delta(e_c)\, 2\pi\, |\langle d|\widehat{V}_{12}|i\rangle|^2 \frac{1}{F_i} \tag{1.33}$$

summing over the polarization and all the magnetic quantum numbers, we finally obtain

$$\sigma^{DR} = \sum_{d} \{ \sum_{m,pol} \frac{(2\pi)^2}{h} \frac{|\langle f|\hat{D}|d\rangle|^2}{\Gamma(d)} \rho_f \, \delta(e_c) \, 2\pi \, |\langle d|\hat{V}_{12}|i\rangle|^2 \frac{1}{F_i} \} \quad (1.34)$$

Using equations (1.26), (1.30), (1.31) and (1.33), equation (1.34) becomes

$$\sigma^{DR} = \sum_{d} \left(\frac{4\pi Ry}{a_0^2 p_c^2}\right) (V_a \, \tau_0) \, \delta(e_c) \, (\pi a_0^2) \quad (1.35)$$

Since there are an infinite number of (d) states in the sum and sometimes a large number of sharp peaks occur around $E_i = E_d$ within a small energy interval, it is convenient to average them over an energy bin of size Δe_c. This energy bin is chosen to be much smaller than the actual experimental beam width but large enough to contain many resonances; otherwise it is arbitrary. The energy averaged cross section is defined as,

$$\bar{\sigma}^{DR} \equiv \frac{1}{\Delta e_c} \int_{e_c - \frac{\Delta e_c}{2}}^{e_c + \frac{\Delta e_c}{2}} \sigma^{DR}(e'_c) \, de'_c \quad (1.36)$$

$$\bar{\sigma}^{DR} = \left(\frac{4\pi \, Ry}{a_0^2 p_c^2 \Delta e_c}\right) V_a(i \rightarrow d) \, \tau_0 \, \omega(d) \, \pi a_0^2 \quad (1.37)$$

where all the quantities in the brackets are dimensionless. Similarly, RE cross section is given by,

$$\bar{\sigma}^{RE} = \left(\frac{4\pi \ Ry}{a_0^2 \ p_c^2 \Delta e_c}\right) V_a(i \rightarrow d) \ \tau_0 \ Z(d) \ \pi a_0^2 \qquad (1.38)$$

The DR (RE) rate coefficient is defined as a thermal average of the DR (RE) cross section

$$\alpha^{DR} = \langle \ v_c \ \sigma^{DR} \ \rangle \qquad (1.39)$$

$$\alpha^{RE} = \langle \ v_c \ \sigma^{RE} \ \rangle \qquad (1.40)$$

where v_c is the continuum electron velocity. If the plasma is in local thermodynamic equilibrium, the projectile electron velocity will have a Maxwellian distribution, thus we can write

$$\alpha^{DR} = \int v_c \ \sigma^{DR} \ d\varphi(e_c) \qquad (1.41)$$

where

$$d\varphi(e_c) = \frac{4\pi}{(2\pi k_B T_e)^{3/2}} e^{-e_c k_B T_e} \ v_c \ de_c \qquad (1.42)$$

Using equations (1.37) and (1.42) in (1.41), we get

$$\alpha^{DR} = \left(\frac{4\pi Ry}{k_B T_e}\right)^{3/2} a_0^3 V_a \omega(d) e^{-e_c k_B T_e} \qquad (1.43)$$

in units of cm^3/sec.

Similarly, the RE rate coefficient is given by,

$$\alpha^{RE} = \left(\frac{4\pi Ry}{k_B T_e}\right)^{3/2} a_0^3 V_a Z(d) e^{-e_c k_B T_e} \qquad (1.44)$$

Comparing equations (1.43) and (1.37), it is clear that σ^{DR} and α^{DR} are related through the following conversion formula,

$$\sigma^{DR} = \{4.06 \times 10^{-9} \left(\frac{k_B T_e}{Ry}\right) e^{-e_c/k_B T_e} \left(\frac{e_c \Delta e_c}{Ry^2}\right)\} \alpha^{DR} \qquad (1.45)$$

This formula is useful in comparing the theoretical estimate with the experimental data on σ^{DR} and α^{DR}.

CHAPTER 2

RESONANT ELASTIC SCATTERING AND ELECTRON CAPTURE BY AL-LIKE P^{2+} AND S^{3+} IONS AT LOW ENERGIES

2.1 Introduction

Resonance excitation which combines both resonant excitation and resonant elastic scattering is the complementary process to dielectronic recombination, and the latter is of major importance in radiation cooling of high-temperature plasma. The probabilities of these processes are related by[9] $P_{DR} + P_{RE} = 1$. In order to make a precise description of the behaviour of such types of plasmas, accurate estimation of the DR, RE and other processes rate coefficients for many different ions is needed.

The dielectronic recombination process involves an initial excitation capture in going from initial state i to intermediate state d, such as

$$(3s^2\ 3p)\ (i) + e \rightarrow (3s\ 3p^2)\ n\ \ell\ (d) \qquad (2.1)$$

this is followed by a radiative decay of the intermediate state d to a final state f,

$$(3s\ 3p^2)\ n\ \ell\ (d) \rightarrow (3s\ 3p^2)\ n'\ \ell'\ (f) + (n\ \ell \rightarrow n'\ \ell') \qquad (2.2)$$

while in the resonance excitation, the initial process is followed by emission of an Auger electron,

$$(3s\ 3p^2\ )\ n\ \ell\ (d) \rightarrow (3s\ 3p^2)\ (f) + e' \qquad (2.3)$$

(Explicit reference to the core electrons of Al-like ions is omitted for simplicity)

In this paper we investigate the intermediate metastable series for Al-like ions such as $(3s\ 3p^2)^4P\ n\ \ell$ which are close to the ground state $(3s^2\ 3p)^2P$. The processes treated in this paper are relatively simple mainly because (i) there is only one Auger channel $(3s\ 3p^2\ n\ \ell \rightarrow 3s^2\ 3p\ k_c\ \ell_c)$, (ii) the radiative transition probabilities (A_r) are dependent on the outer electron due to the forbidden transition of the core, this means that high Rydberg states contribution ($n > 30$) are small and negligible because of the well known scaling of A_r, $A_r\ \alpha\ 1/n^3$.

In section II we briefly summarize the theoretical procedure employed in the evaluation of the DR and RES

cross sections and rate coefficients. In section III we present the results of our data, followed by a conclusion in section IV.

2.2 Theoretical Procedure

The details of the theoretical procedure used in the present work are covered in full in previous publication by Hahn[3], and Hahn and LaGattuta[10]. Therefore, only a brief summary of the main assumptions is presented.

Define an energy-averaged[11] cross sections $\bar{\sigma}^{DR}$, and $\bar{\sigma}^{RES}$

$$\bar{\sigma}^{DR} \equiv \frac{1}{\Delta e_c}\int_{e_c-\frac{\Delta e_c}{2}}^{e_c+\frac{\Delta e_c}{2}} \sigma^{DR}(e_c')\, de_c' \tag{2.4}$$

$$\bar{\sigma}^{RES} \equiv \frac{1}{\Delta e_c}\int_{e_c-\frac{\Delta e_c}{2}}^{e_c+\frac{\Delta e_c}{2}} \sigma^{RES}(e_c')\, de_c' \tag{2.5}$$

$$\bar{\sigma}^{DR} = \frac{4\pi(Ry)}{e_c(Ry)}\,\tau_0\, V_a(i\rightarrow d)\,\omega(d)\,\frac{1}{\Delta e_c}(\pi\, a_0^2) \tag{2.6}$$

$$\bar{\sigma}^{RES} = \frac{4\pi(Ry)}{e_c(Ry)}\,\tau_0\, V_a(i\rightarrow d)\, Z(d)\,\frac{1}{\Delta e_c}(\pi\, a_0^2) \tag{2.7}$$

where V_a is the radiationless excitation capture probability which is related, by detailed balance[12], to the Auger emission probability $A_a(d\rightarrow i)$ by $V_a = (g_d/2g_i)\, A_a(d\rightarrow i)$, where g_d and g_i are statistical weights of the intermediate and initial states , respectively. a_0 and τ_0 are the Bohr radius and atomic unit of time. Δe_c is a small energy bin which is chosen arbitrary but with the requirement that it is small compared with the actual experimental continuum electron beam width. $Z(d) = A_a(d\rightarrow i)/\Gamma(d)$ and $\omega(d\rightarrow f) = A_r(d\rightarrow f)/\Gamma(d)$ are the partial Auger and fluorescence yields of the state d, respectively. A_r is the radiative transition probability. $\Gamma(d) = \Sigma_i\, A_a(d\rightarrow i) + \Sigma_f\, A_r(d\rightarrow f)$ is the total width of the intermediate state. In general, the rates $\bar{\alpha}^{DR}$, and $\bar{\alpha}^{RES}$ are given by[11],

$$\bar{\alpha}^{DR} = \left(\frac{4\pi(Ry)}{kT(Ry)}\right)^{3/2} a_0^3\, V_a(i\rightarrow d)\, \omega(d)\, e^{-e_c/kT} \qquad (2.8)$$

$$\bar{\alpha}^{RES} = \left(\frac{4\pi\,(Ry)}{kT\,(Ry)}\right)^{\frac{3}{2}} a_0^3\, V_a\,(i\rightarrow d)\, Z(d)\, e^{-e_c/kT} \qquad (2.9)$$

In general, the cross sections $\bar{\sigma}^{DR}$, $\bar{\sigma}^{RES}$ and the rates $\bar{\alpha}^{DR}$, $\bar{\alpha}^{RES}$ are related by[10]

$$\bar{\sigma}^{DR} = (4.06\times 10^{-9})\, \frac{kT}{(Ry)^{3/2}}\, \frac{e^{e_c/kT}}{e_c\, \Delta e_c}\, \bar{\alpha}^{DR} \qquad (2.10)$$

$$\bar{\sigma}^{RES} = (4.06 \times 10^{-9}) \frac{kT}{(Ry)^{3/2}} \frac{e^{e_c/kT}}{e_c \Delta e_c} \bar{\alpha}^{RES} \qquad (2.11)$$

Cowan's code, in single-configuration Hartree-Fock approximation and in full LS coupling, was used in the calculation of the transition energies as well as the relevant A_a and A_r needed in the evaluation of the DR and RES cross sections. Data tables[13] were used to adjust energies, wherever possible. This is important especially when the transition energies are small. Cowan's code was used to evaluate energy levels for all intermediate states with $n < 10$. Auger transition probabilities, A_a require both bound and continuum wavefunctions. The continuum wavefunctions were generated[3,10] by a distorted-wave method using the Hartree-Fock potential.

2.3 Results and Discussion

DR and RES cross sections and rate coefficients for Al-like P^{2+} and S^{3+} ions for the intermediate metastable state series $(3s\ 3p^2)^4P\ n\ \ell$ were evaluated in LS coupling. The cross sections $\bar{\sigma}^{DR}(cm^2)$ and $\bar{\sigma}^{RES}(cm^2)$ for P^{2+} are given in table 1 as functions of $e_c(Ry)$. As shown in table 1, $\bar{\sigma}^{RES}$ are greater than $\bar{\sigma}^{DR}$ by a factor of 10^6. For S^{3+} ion, the cross sections

$\overline{\sigma}^{DR}(cm^2)$ and $\overline{\sigma}^{RES}(cm^2)$ are tabulated in table 2, the $\overline{\sigma}^{RES}$ is still larger than $\overline{\sigma}^{DR}$ by a factor of 10^4. In figures 1 and 2, the $\log_{10}\overline{\alpha}^{DR}(cm^3/sec)$ and $\log_{10}\overline{\alpha}^{RES}(cm^3/sec)$ for P^{2+} and S^{3+} are plotted as functions of $\log_{10}kT(Ry)$. For P^{2+} the rates peak near kT = 0.001 Ry, with the values 0.25×10^{-12} cm^3/sec , and 0.48×10^{-6} cm^3/sec for DR and RES , respectively. For S^{3+} the rates peak near kT = 0.01 Ry, with the values 0.82×10^{-12} cm^3/sec and 0.11×10^{-7} cm^3/sec for DR and RES, respectively. The rate coefficients of P^{2+} are decaying much faster than those of S^{3+}. The sudden drop in the DR cross sections of P^{2+} at the continuum energies e_c = 0.26 and 0.35 Ry, are mainly due to the smallness of the radiative transitions probability of the intermediate states (3s $3p^2$) 4f and (3s $3p^2$) 5f, respectively.

Due to the unitary nature of the mixing matrix, the total cross sections are generally much less sensitive to the mixing (in order of ±10% change), although the individual states are sometimes very much affected by it. The dependence of our results on the coupling scheme used is also very weak in so far as the total is concerned. That is why we neglected these and other possible complications in the present calculations.

2.4 Conclusion

We have calculated DR and RES cross sections and rate coefficients for intermediate metastable state series $(3s\ 3p^2)^4P\ n\ \ell$ of Al-like P^{2+} and S^{3+}. Explicit cross sections are listed in tables 1 and 2 as functions of e_c(Ry). Figures 1 and 2 display $\log_{10}\overline{\alpha}^{DR}(cm^3/sec)$ and $\log_{10}\overline{\alpha}^{RES}(cm^3/sec)$ as functions of $\log_{10}$kT(Ry) for P^{2+} and S^{3+}, respectively. The RES are larger than DR by an order of magnitude $10^4 \sim 10^6$. DR cross sections and rates increase with increasing atomic number in a given isoelectronic sequence, unlike in DR, the RES cross sections and rates decrease with increasing atomic number in a given isoelectronic sequence. A similar work for DR and RE is in progress to study the main behaviour of the cross sections and rates for different ions in Al-like sequence.

Table 2.1. Values of $\bar{\sigma}^{DR}(cm^2)$ and $\bar{\sigma}^{RES}(cm^2)$ as functions of electron energies e_c(Ry) for the intermediate metastable series $(3s\ 3p^2)^4P\ n\ \ell$ of P^{2+}, Δe_c = 0.01 Ry. Powers of 10 are shown in parenthesis

e_c(Ry)	$\bar{\sigma}^{DR}(cm^2)$	$\bar{\sigma}^{RES}(cm^2)$
0.01	3.20(-20)	5.98(-14)
0.19	3.45(-21)	1.44(-15)
0.21	1.36(-20)	1.51(-15)
0.24	1.13(-21)	1.25(-15)
0.26	1.82(-28)	1.86(-17)
0.32	1.02(-21)	3.58(-16)
0.33	3.05(-21)	5.08(-16)
0.34	4.55(-22)	4.05(-16)
0.35	4.87(-29)	1.13(-17)
0.38	5.57(-22)	1.54(-16)
0.39	1.49(-21)	2.40(-16)
0.40	2.49(-22)	1.97(-16)
0.42	1.19(-21)	2.17(-16)
0.43	1.55(-22)	1.11(-16)
0.44	9.24(-22)	1.69(-16)
0.45	4.36(-22)	2.00(-16)
0.46	8.81(-22)	1.84(-16)
0.47	6.09(-22)	1.45(-16)
0.48	5.50(-22)	1.36(-16)
0.49	3.62(-22)	6.58(-17)
0.50	1.05(-22)	1.67(-17)
Total	6.22(-20)	6.71(-14)

Table 2.2. Values of $\bar{\sigma}^{DR}(cm^2)$ and $\bar{\sigma}^{RES}(cm^2)$ as functions of electron energies $e_c(Ry)$ for the intermediate metastable series $(3s\ 3p^2)^4P\ n\ \ell$ of S^{3+}.

$e_c(Ry)$	$\bar{\sigma}^{DR}(cm^2)$	$\bar{\sigma}^{RES}(cm^2)$
0.06	1.96(-19)	1.95(-16)
0.10	1.73(-20)	2.43(-15)
0.23	2.96(-21)	7.86(-16)
0.25	4.71(-21)	5.05(-16)
0.28	2.87(-20)	3.86(-17)
0.30	3.33(-21)	3.76(-16)
0.37	5.28(-22)	2.58(-16)
0.38	1.87(-21)	1.75(-16)
0.39	1.23(-20)	1.97(-17)
0.40	1.51(-21)	1.49(-16)
0.44	4.41(-25)	1.24(-16)
0.45	1.05(-21)	8.61(-17)
0.46	6.72(-21)	1.18(-17)
0.47	8.72(-22)	7.82(-17)
0.49	2.67(-25)	7.08(-17)
0.50	4.77(-21)	5.89(-17)
0.51	1.03(-21)	8.21(-17)
0.52	3.94(-22)	3.28(-17)
0.53	3.07(-21)	7.58(-17)
0.54	5.45(-22)	7.47(-17)
0.55	2.49(-21)	7.16(-17)
0.56	1.93(-21)	4.51(-17)
0.57	1.38(-21)	4.47(-17)
0.58	1.24(-21)	5.88(-17)
0.59	1.07(-21)	5.03(-17)
0.60	1.60(-21)	4.18(-17)
0.61	8.67(-22)	2.56(-17)
0.62	9.70(-22)	1.71(-17)
0.63	9.54(-22)	7.53(-18)
0.64	6.49(-23)	1.27(-19)
Total	3.01(-19)	5.99(-15)

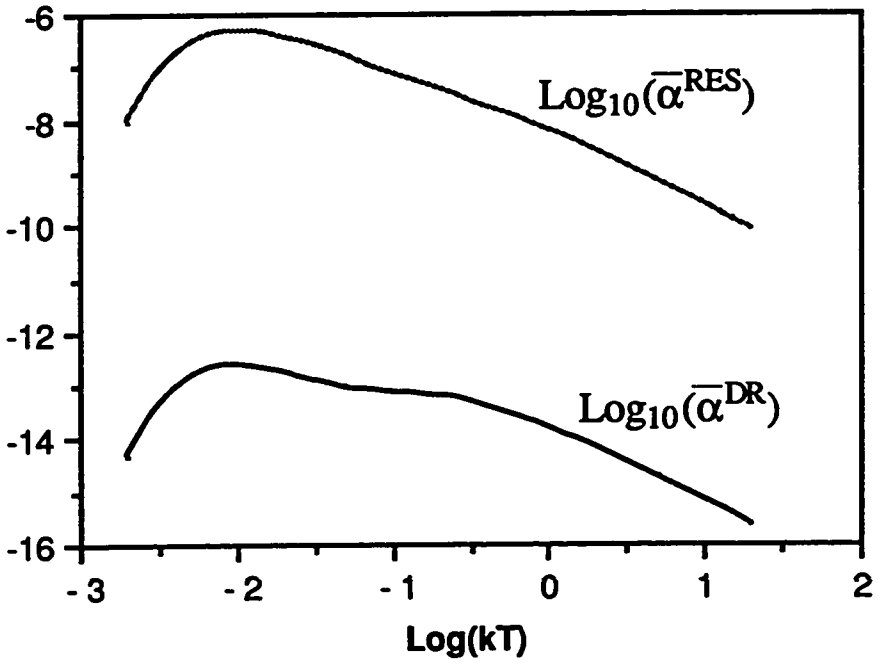

Figure 2.1. $Log_{10}\,\bar{\alpha}^{DR}(cm^3/sec)$ and $log_{10}\,\bar{\alpha}^{RES}(cm^3/sec)$ as funcitons of $log_{10}kT(Ry)$ for P^{2+}.

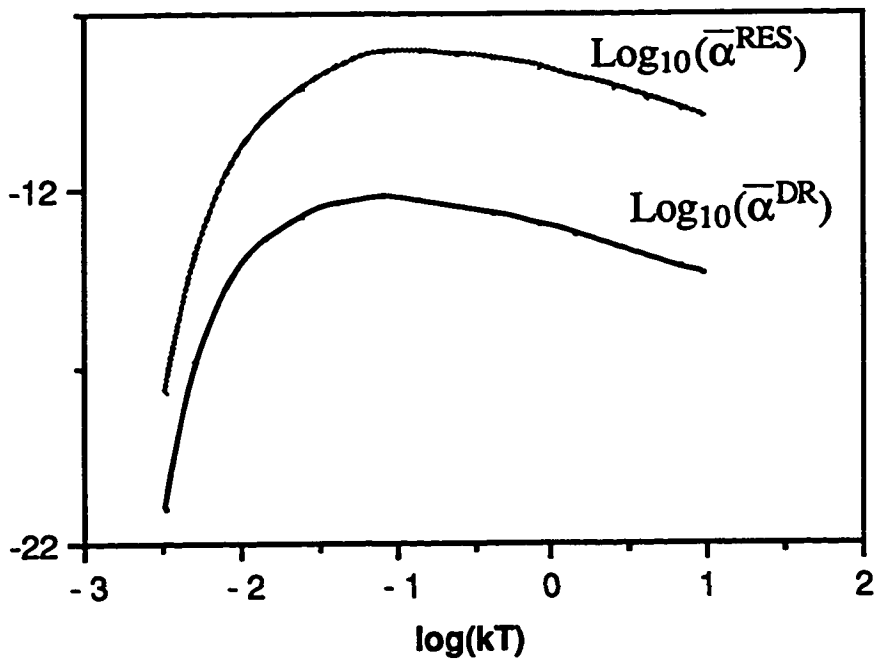

Figure 2.2. $Log_{10}\bar{\alpha}^{DR}(cm^3/sec)$ and $log_{10}\bar{\alpha}^{RES}(cm^3/sec)$ as funcitons of $log_{10}kT(Ry)$ for S^{3+}.

CHAPTER 3

DIELECTRONIC RECOMBINATION CROSS SECTIONS AND RATE COEFFICIENTS FOR S^{3+}

Electron capture by ionic targets ($A^{z+} = i$) with a degree of ionization z via intermediate resonance states (($A^{(z-1)+}$)** = d), followed by stabilizing radiation emission to a final state (($A^{(z-1)+}$)* = f) is known as dielectronic recombination (DR) process[14,15]. It is an important tool by which astronomical and laboratory high-temperature plasmas cool radiatively. Accurate estimation of the rate coefficients of processes like DR for many different ions is essential to make precise description of the behavior of such types of plasmas. There has been much interest in measuring the oxygen to sulfur ratio in Jupiter's plasma torus[16]. The method of measurement depends on ion emissions in the torus. Knowing the rate coefficients of the different ions involved is important to make acceptable measurement of the ratio. In more recent theoretical work done by Badnell[17] for S^{q+}, he used LS coupling incorporated with configuration mixing to the N-electron core. In this report we present our results of estimating DR cross sections and rate coefficients of Al-like S^{3+} for the process in which the 3s electron is excited

to the 3p state and the projectile electron is captured to high Rydberg state (n ℓ) using single-configuration and non-relativistic Hartree-Fock wavefunction in LS coupling scheme. The DR process could, simply, be represented, in $\Delta n = 0$, $\Delta \ell = 1$ mode of excitation, by,

$$(3s^2 3p = i) + k_c \ell_c \rightarrow (3s3p^2\ n\ell = d) \rightarrow (3s3p^2\ n'\ell = f) + \gamma(n\ell \rightarrow n'\ell') \tag{3.1}$$

with an extra Auger channel $\Delta n = 0$, $\Delta \ell = 0$ mode, due to the multiplets of the first excited state ($3s\ 3p^2$), i.e.

$$(3s3p^2 = i') + k_c' \ell_c' \rightarrow (3s3p^2\ n\ell = d) \rightarrow (3s3p^2\ n'\ell = f) + \gamma(n\ell \rightarrow n'\ell') \tag{3.2}$$

[Explicit reference to the core electrons and multiplets of the excited states of Al-like ions is omitted for simplicity]

The theoretical procedure is similar to that of chapter 2. Define the sum of the cross sections as,

$$S = \bar{\sigma}_{tot}^{DR}(i) = \Sigma_n \Sigma_d\ \bar{\sigma}^{DR}(i) \tag{3.3}$$

We used Cowan's code[18], in single-configuration and non-relativistic Hartree-Fock approximation and in LS coupling scheme, in the evaluation of the transition energies as well as

the relevant A_a and A_r used in the estimation of the DR cross sections. Data tables[13] were consulted to adjust energies, wherever possible.

For convenience, we define the various channels needed in our work as,

$$i_1 = (3s^2 3p)^2P$$
$$i_2 = (3s3p^2)^4P \qquad d_1 = (i_2)\ n\ \ell$$
$$i_3 = (3s3p^2)^2D \qquad d_2 = (i_3)\ n\ \ell$$
$$i_4 = (3s3p^2)^2S \qquad d_3 = (i_4)\ n\ \ell$$
$$i_5 = (3s3p^2)^2P \qquad d_4 = (i_5)\ n\ \ell$$

In fig. 1 the energy levels relevant to DR process for S^{3+} ion are given, from which all possible radiative and Auger transitions for the individual intermediate resonance states may be determined. Energy differences and the radiative transition probabilities of the ionic core involved are shown in table 1, and these are the dominant radiative decay rates for large n. The cross sections $\bar{\sigma}^{DR}(cm^2)$ as functions of electron energies e_c(Ry) for the ground state i_1 are tabulated in table 2, and the explicit contributions of each intermediate state series are also given. Cross sections $\bar{\sigma}^{DR}(cm^2)$ for the initial states i_2 , i_3 , and i_4 as functions of e_c(Ry) are tabulated in table 3. It is important to estimate the contributions from excited states[19] eventhough some

states are not able to radiatively stabilize such as i_3 and i_4, but the metastable state i_2 is usually present in the ion beam with unknown percentage (maybe 50%)[20,21]. As shown in table 3, the contribution of the metastable state i_2 is about 10% of i_1, and this may affect the overall distribution of the rates and cross sections at small values of e_c, $e_c \leq 0.55$ Ry. In $\Delta n = 0$, $\Delta \ell = 1$ mode we compared our results for the rate coefficients with those given by Badnell[17] and Jacobs et. al.[22] in table 4 and it was found that our results as well as those of Badnell and Jacobs peak at kT = 0.79 (Ry) which is 2/3 of the energy gap between i_1 and i_5. This peak is mainly due to d_2 and d_4 series. There is a factor of 1.08 of Badnell[17] results to ours at the temperature of the peak. This difference may be due to the configuration mixing he used in the core. Although Jacobs et. al.[22] imposed a cutoff on n given by the Inglis-Teller criteria, his results are 1.13 times larger than our results, this is because he neglected the nondipole autoionization, which when included will increase the total width of the intermediate state, i.e. will decrease their cross sections and rates by 15%. DR rate coefficients $\overline{\alpha}^{DR}(cm^3/sec)$ as functions of kT(Ry) for multiplet transitions are tabulated in table 5. For convenience, multiplet transition DR cross sections $\overline{\sigma}^{DR}(cm^2)$ in $\Delta n = 0$, $\Delta \ell = 1$ mode of excitation are given in table 6 as functions of n.

Finally, we can conclude that the configuration mixing of the ion core is small for this ion, i.e. S^{3+}, and also the contribution of the metastable state i_2 could affect the overall distribution at small e_c, $e_c \leq 0.55$ Ry.

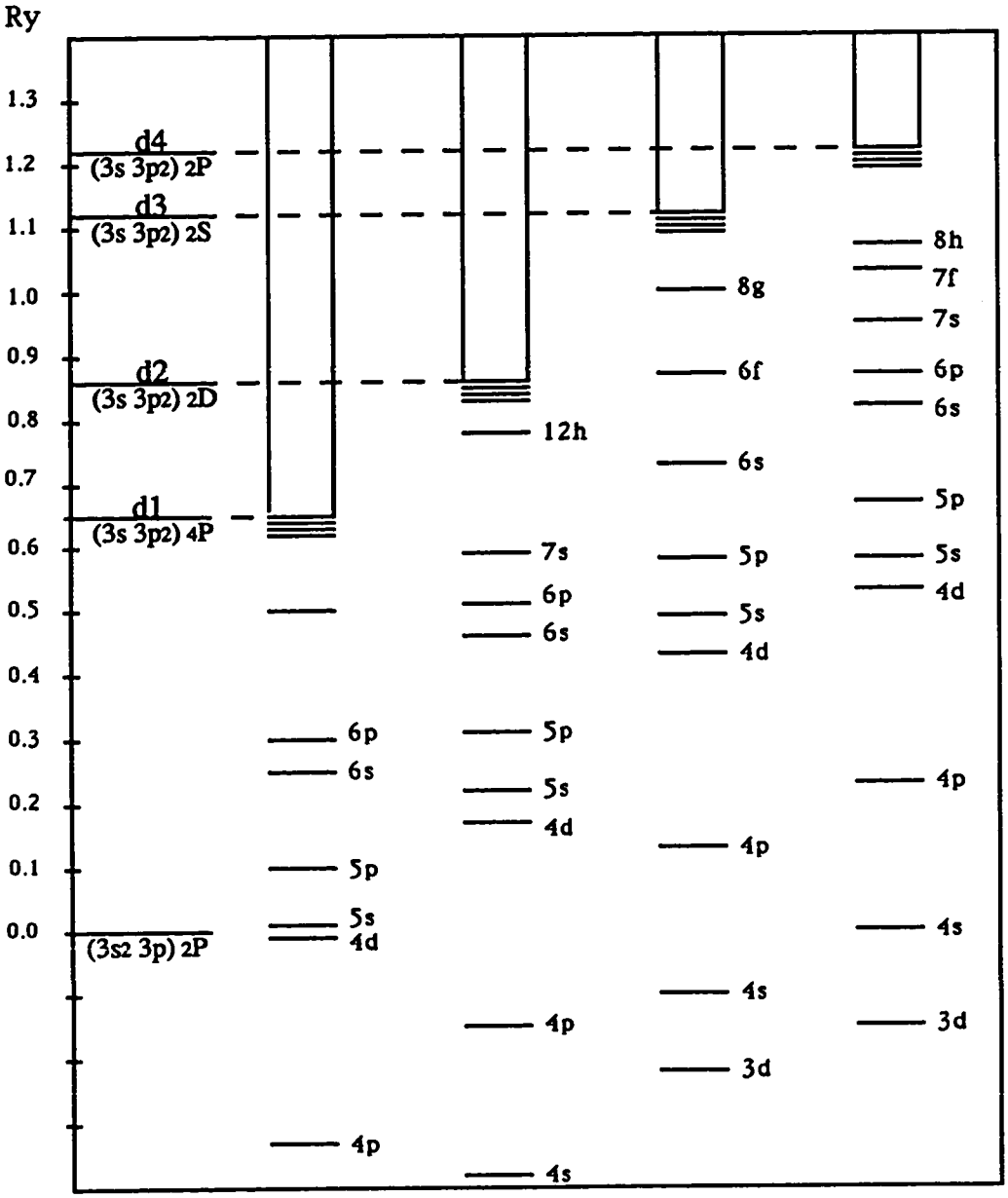

Figure 3.1. Energy level diagram of S^{3+} ion showing relevant levels to DR process, from which all possible radiative and Auger transitions for the idividual intermediate resonance states may be determined.

Table 3.1. Energy differences of S^{3+} ionic core and their dominant radiative decay rates A_r.

i	ΔE(Ry)	$A_r(sec^{-1})$
$i_1 = (3s^2\ 3p)^2P$	0	0
$i_2 = (3s\ 3p^2)^4P$	0.652	0
$i_3 = (3s\ 3p^2)^2D$	0.858	1.43(+09)
$i_4 = (3s\ 3p^2)^2S$	1.130	3.08(+09)
$i_5 = (3s\ 3p^2)^2P$	1.220	1.20(+10)

Table 3.2. DR cross sections $\bar{\sigma}^{DR}(cm^2)$ as functions of electron energies e_c(Ry) for the ground state i_1, with $\Delta e_c = 0.01$ Ry. Explicit contributions from the intermediate states d_1, d_2, d_3 and d_4 are given.

e_c	^4P	^2D	^2S	^2P
0.06	1.96(-19)			
0.10	1.73(-20)			
0.17		2.91(-19)		
0.21		7.21(-20)		
0.23	2.96(-21)			
0.25	4.71(-21)			
0.27		4.18(-19)		
0.28	2.87(-20)			
0.30	3.33(-21)	8.56(-20)		
0.37	5.28(-22)			
0.38	1.87(-21)			
0.39	1.23(-20)			
0.40	1.51(-21)			
0.44	4.41(-25)	8.62(-20)	3.47(-20)	
0.45	1.05(-21)			
0.46	6.72(-21)	2.40(-20)		
0.47	8.72(-22)			
0.48		1.75(-19)	9.54(-21)	
0.49	2.67(-25)	1.08(-19)		
0.50	4.77(-21)	4.88(-20)		
0.51	1.03(-21)			
0.52	3.94(-22)			
0.53	3.07(-21)			3.40(-19)
0.54	5.45(-22)		5.70(-20)	
0.55	2.49(-21)			
0.56	1.93(-21)			
0.57	1.38(-21)	6.64(-20)		7.82(-20)
0.58	1.24(-21)	1.61(-20)	4.89(-21)	
0.59	1.07(-21)			
0.60	1.59(-21)	3.22(-19)		
0.61	8.51(-22)	3.91(-20)		
0.62	9.70(-22)			
0.63	9.42(-22)			5.12(-19)

Table 3.2. continued.

e_c	^4P	^2D	^2S	^2P
0.65		3.83(-20)		
0.66		8.95(-21)		
0.67		4.05(-19)		1.55(-19)
0.68				
0.69				
0.70		3.72(-20)		
0.71		4.44(-19)	1.40(-20)	
0.72		2.00(-20)		
0.73		3.56(-20)	4.84(-21)	
0.74		5.58(-19)		
0.75		6.06(-20)		
0.76		5.50(-19)	6.48(-20)	
0.77		5.83(-20)	9.72(-21)	
0.78		5.96(-19)		
0.79		1.07(-18)		
0.80		1.36(-18)		1.96(-19)
0.81		2.43(-18)		
0.82		4.47(-18)		4.71(-20)
0.83		5.15(-18)		
0.84		2.07(-17)	1.23(-20)	
0.85			2.00(-21)	6.53(-19)
0.86				1.10(-19)
0.87			3.12(-20)	
0.88			1.58(-20)	
0.90				
0.91				
0.92			3.96(-21)	
0.93			1.55(-21)	1.83(-19)
0.94			5.68(-20)	3.86(-20)
0.95			4.38(-21)	
0.96				5.53(-19)
0.97			3.67(-21)	4.00(-19)
0.98			7.79(-20)	
0.99			4.24(-21)	
1.00			1.45(-21)	

Table 3.2. continued.

θ_c	^4P	^2D	^2S	^2P
1.01			1.45(-21)	8.59(-20)
1.02			2.04(-20)	2.92(-20)
1.03			8.79(-20)	1.22(-18)
1.04			2.28(-20)	7.60(-20)
1.05			1.27(-19)	
1.06			1.56(-19)	1.15(-19)
1.07			2.99(-19)	2.21(-19)
1.08			2.01(-19)	1.28(-18)
1.09			5.67(-19)	2.74(-20)
1.10			1.11(-18)	3.99(-19)
1.11			8.35(-19)	1.50(-18)
1.12			4.21(-18)	4.45(-19)
1.13			1.03(-18)	1.79(-18)
1.14				1.87(-18)
1.15				3.51(-18)
1.16				2.71(-18)
1.17				6.92(-18)
1.18				1.33(-17)
1.19				1.04(-17)
1.20				4.54(-17)
1.21				8.53(-18)
Total	3.00(-19)	3.97(-17)	9.09(-18)	1.03(-16)

Table 3.3. DR cross sections $\bar{\sigma}^{DR}(cm^2)$ as functions of electron energies e_c(Ry) for the excited states i_2, i_3 and i_4.

e_c	^4P	^2D	^2S
0.01	3.54(-19)	3.24(-19)	1.46(-18)
0.02	1.41(-19)	9.72(-19)	5.46(-19)
0.03			7.06(-19)
0.04			1.07(-18)
0.05	8.57(-20)		2.09(-18)
0.06	1.26(-19)	7.32(-20)	9.49(-18)
0.07	2.68(-21)	1.03(-20)	8.35(-18)
0.08	7.56(-20)	6.17(-19)	
0.09	4.20(-20)	2.96(-20)	
0.10	1.00(-19)	6.66(-20)	
0.11	7.38(-20)	9.34(-20)	
0.12	7.64(-20)	4.00(-20)	
0.13	1.25(-19)	3.25(-19)	
0.14	1.92(-19)	5.44(-21)	
0.15	5.92(-19)	2.21(-19)	
0.16	2.97(-18)	3.33(-19)	
0.17	3.51(-19)	1.11(-19)	
0.18	3.66(-18)	3.99(-19)	
0.19	1.29(-18)	3.06(-19)	
0.20	1.95(-23)	4.91(-19)	
0.21	2.39(-20)	6.50(-19)	
0.22	1.37(-21)	1.17(-18)	
0.23	1.52(-21)	2.07(-18)	
0.24		1.86(-18)	
0.25		6.69(-18)	
0.26		4.81(-18)	
0.27	3.08(-21)	1.26(-19)	
0.28	3.82(-20)	4.93(-20)	
0.29	5.29(-21)	2.38(-19)	
0.30		2.03(-19)	
0.31	9.59(-21)	5.60(-19)	
0.32	1.83(-20)	1.80(-18)	
0.33	8.20(-22)	1.00(-18)	
0.34	9.85(-22)	3.18(-18)	
0.35	2.19(-21)	3.96(-19)	

Table 3.3. continued.

e_c	^4P	^2D	^2S
0.36	6.92(-20)		
0.37	4.91(-21)		
0.38	2.25(-20)		
0.39	2.81(-21)		
0.40	6.12(-21)		
0.41	2.82(-20)		
0.42	1.68(-20)		
0.43	4.83(-20)		
0.44	1.49(-19)		
0.45	2.60(-19)		
0.46	1.18(-19)		
0.47	2.39(-20)		
0.48	2.77(-20)		
0.49	5.46(-20)		
0.50	6.84(-20)		
0.51	1.80(-19)		
0.52	3.91(-19)		
0.53	4.19(-19)		
0.54	6.84(-19)		
0.55	2.33(-19)		
Total	1.32(-17)	2.93(-17)	2.37(-17)

Table 3.4. Rate coefficients $\bar{\alpha}^{DR}(cm^3/sec)$ as functions of kT(Ry) for the ground state i_1 are compared with those obtained by Badnell[17] and Jacobs et. al.[22].
* These figures were extrapolated.

kT(Ry)	^4P	^2D	^2S	^2P	Total	Badnell	Jacobs
0.10(+00)	0.65(-12)	0.23(-11)	0.43(-13)	0.21(-12)	3.2(-12)		4.9(-12)
0.20(+00)	0.42(-12)	0.16(-10)	0.12(-11)	0.99(-11)	2.8(-11)	2.9(-11)	1.0(-11)
0.25(+00)	0.36(-12)	0.25(-10)	0.25(-11)	0.22(-10)	5.0(-11)	4.8(-11)	3.8(-11)
0.30(+00)	0.31(-12)	0.32(-10)	0.39(-11)	0.36(-10)	7.2(-11)	7.7(-11)	8.5(-11)*
0.39(+00)	0.25(-12)	0.40(-10)	0.61(-11)	0.60(-10)	1.1(-10)	1.1(-10)	1.0(-10)
0.50(+00)	0.19(-12)	0.43(-10)	0.77(-11)	0.80(-10)	1.3(-10)	1.4(-10)	1.4(-10)*
0.60(+00)	0.16(-12)	0.43(-10)	0.85(-11)	0.90(-10)	1.4(-10)	1.6(-10)	1.6(-10)
0.79(+00)	0.12(-12)	0.40(-10)	0.87(-11)	0.95(-10)	1.5(-10)	1.6(-10)	1.7(-10)*
0.99(+00)	0.91(-13)	0.35(-10)	0.82(-11)	0.92(-10)	1.4(-10)	1.6(-10)	1.6(-10)
0.12(+01)	0.71(-13)	0.30(-10)	0.75(-11)	0.85(-10)	1.2(-10)	1.4(-10)	1.5(-10)*
0.16(+01)	0.49(-13)	0.24(-10)	0.61(-11)	0.71(-10)	1.0(-10)	1.2(-10)	1.3(-10)
0.20(+01)	0.37(-13)	0.19(-10)	0.50(-11)	0.59(-10)	8.3(-11)	1.0(-10)	1.1(-10)*
0.25(+01)	0.27(-13)	0.15(-10)	0.40(-11)	0.47(-10)	6.6(-11)	8.0(-11)	8.7(-11)
0.31(+01)	0.20(-13)	0.11(-10)	0.32(-11)	0.37(-10)	5.1(-11)	6.3(-11)	7.0(-11)*
0.39(+01)	0.14(-13)	0.84(-11)	0.24(-11)	0.29(-10)	4.0(-11)	4.8(-11)	5.2(-11)
0.50(+01)	0.10(-13)	0.61(-11)	0.18(-11)	0.21(-10)	2.9(-11)	3.6(-11)	4.1(-11)*
0.63(+01)	0.73(-14)	0.44(-11)	0.13(-11)	0.16(-10)	2.2(-11)	2.7(-11)	2.9(-11)
0.80(+01)	0.51(-14)	0.32(-11)	0.95(-12)	0.11(-10)	1.5(-11)		1.6(-11)
0.10(+02)	0.37(-14)	0.23(-11)	0.70(-12)	0.84(-11)	1.1(-11)		
0.12(+02)	0.28(-14)	0.18(-11)	0.54(-12)	0.65(-11)	8.8(-12)		

Table 3.5. Rate coefficients $\bar{\alpha}^{DR}(cm^3/sec)$ as functions of kT(Ry) for the excited states i_2, i_3 and i_4.

kT(Ry)	^4P	^2D	^2S
0.40(-02)	9.1(-13)	1.9(-12)	3.2(-12)
0.60(-02)	2.4(-12)	5.0(-12)	6.9(-12)
0.80(-02)	3.5(-12)	7.2(-12)	1.0(-11)
0.10(-01)	4.1(-12)	8.5(-12)	1.5(-11)
0.30(-01)	5.8(-12)	9.4(-12)	7.3(-11)
0.50(-01)	1.2(-11)	1.6(-11)	8.6(-11)
0.80(-01)	2.1(-11)	3.3(-11)	7.3(-11)
0.10(+00)	2.4(-11)	4.2(-11)	6.2(-11)
0.30(+00)	1.8(-11)	4.5(-11)	2.0(-11)
0.50(+00)	1.2(-11)	3.0(-11)	1.0(-11)
0.80(+00)	7.6(-12)	1.8(-11)	5.3(-12)
0.10(+01)	5.8(-12)	1.4(-11)	3.8(-12)
0.30(+01)	1.4(-12)	3.3(-12)	7.8(-13)
0.50(+01)	6.7(-13)	1.6(-12)	3.6(-13)
0.80(+01)	3.5(-13)	7.9(-13)	1.8(-13)
0.10(+02)	2.4(-13)	5.8(-13)	1.3(-13)
0.12(+02)	1.9(-13)	4.4(-13)	9.9(-14)
0.15(+02)	1.4(-13)	3.1(-13)	7.1(-14)

Table 3.6. DR cross sections $\bar{\sigma}^{DR}(cm^2)$ as functions of n in $\Delta n = 0$, $\Delta \ell = 1$ mode of excitation for the ground state i_1, with $\Delta e_c = 0.01$ Ry.

n	^4P	^2D	^2S	^2P
4	1.96(-19)	7.09(-19)	9.18(-20)	8.52(-19)
5	4.89(-20)	5.27(-19)	9.32(-20)	1.08(-18)
6	2.09(-20)	4.61(-19)	6.92(-20)	1.20(-18)
7	1.01(-20)	4.77(-19)	6.74(-20)	1.45(-18)
8	6.02(-21)	5.03(-19)	8.60(-20)	1.62(-18)
9	3.96(-21)	5.87(-19)	1.08(-19)	1.90(-18)
10	2.78(-21)	5.60(-19)	1.29(-19)	1.83(-18)
11-15	6.00(-21)	2.54(-18)	7.15(-19)	8.28(-18)
16-20	3.00(-21)	2.22(-18)	6.40(-19)	7.20(-18)
21-25	1.00(-21)	2.02(-18)	5.50(-19)	6.20(-18)
26-30		1.70(-18)	4.70(-19)	5.50(-18)
31-40		3.10(-18)	7.80(-19)	9.30(-18)
41-50		2.50(-18)	6.10(-19)	7.60(-18)
51-60		2.00(-19)	5.00(-19)	6.30(-18)
61-70		1.90(-18)	4.40(-19)	5.50(-18)
71-80		1.60(-18)	3.80(-19)	4.60(-18)
81-90		1.50(-18)	3.30(-19)	4.00(-18)
91-100		1.30(-18)	3.00(-19)	3.50(-18)
101-∞		1.33(-17)	2.63(-18)	2.51(-17)

CHAPTER 4

RESONANCE EXCITATION CROSS SECTIONS AND RATE COEFFICIENTS OF S IV ION AT LOW ENERGIES

4.1 Introduction

Resonance excitation which combines both resonance excitation and resonance elastic scattering is the complementary process to dielectronic recombination, and the latter is a very important mechanism by which high-temperature plasmas cool radiatively. The probabilities of these processes are related by[9] $P_{DR} + P_{RE} = 1$. In order to be able to control such types of plasmas, accurate estimation of the DR, RE and other processes cross sections for many different ions is needed.

The dielectronic recombination process involves an initial excitation capture in going from initial state i to intermediate state d, such as

$$(3s^2\ 3p)\ (i) + e \rightarrow (3s\ 3p^2)\ n\ \ell\ (d) \qquad (4.1)$$

this is followed by a radiative decay of the intermediate

state d to a final state f,

$$(3s\ 3p^2)\ n\ \ell\ (d) \rightarrow (3s\ 3p^2)\ n'\ \ell'\ (f) + (n\ \ell \rightarrow n'\ \ell') \quad (4.2)$$

while in the resonance excitation, the initial process is followed by emission of an Auger electron,

$$(3s\ 3p^2\ )\ n\ \ell\ (d) \rightarrow (3s\ 3p^2)\ (f) + e' \quad (4.3)$$

(Explicit reference to the core electrons and the multiplet states of Al-like ions is omitted for simplicity)

In this paper we present our measurement of the dielectronic recombination and resonance excitation cross sections of Al-like S^{3+}.

In section II we briefly summarize the theoretical procedure employed in the evaluation of the DR and RE cross sections and rate coefficients. In section III we present the results of our data, followed by a conclusion in section IV.

4.2. Theoretical Procedure

The theortical procedure is similar to that of chapter 3.

4.3. Results and Discussion

DR and RE cross sections of S^{3+} ion for the multiplets of the first excited state ($3s\ 3p^2$) were evaluated in LS coupling. The cross sections $\overline{\sigma}^{DR}(cm^2)$ and $\overline{\sigma}^{RE}(cm^2)$ for S^{3+} are given in tables 1-10 as functions of e_c(Ry). It can be seen that cross sections due to resonant elastic scattering are dominant with peak value of 4.81×10^{-14} (cm^2) for the transition $i_1 \rightarrow d_2 \rightarrow i_1$. DR cross sections, on the other side, are the least dominant with the highest value of 1.03×10^{-16} (cm^2) for the transition $i_1 \rightarrow d_4$, and least value of 6.03×10^{-19} (cm^2) for the transition $d_1 \rightarrow d_3$. $\overline{\sigma}^{DR}(cm^2)$ and $\overline{\sigma}^{RE}(cm^2)$ as functions of ℓ are tabulated in tables 11-20. $\overline{\alpha}^{DR}(cm^3/sec)$, and $\overline{\alpha}^{RES}(cm^3/sec)$ as functions of kT(Ry) are tabulated in tables 21-30. Rate coefficients for the transitions resulting in i_1 in the final state are the dominant ones[23].

4.4. Conclusion

We have calculated DR and RE cross sections for the multiplets of the first excited state ($3s\ 3p^2$) of Al-like S^{3+}. Explicit cross sections are listed in tables 1-10 as a functions of e_c(Ry). We observe that resonant elastic scattering cross sections are dominant over RE and they are larger than DR by an order of magnitude 10^3. Rate coefficients for transitions resulting in i_1 in the final state are dominant over other RE coefficients.

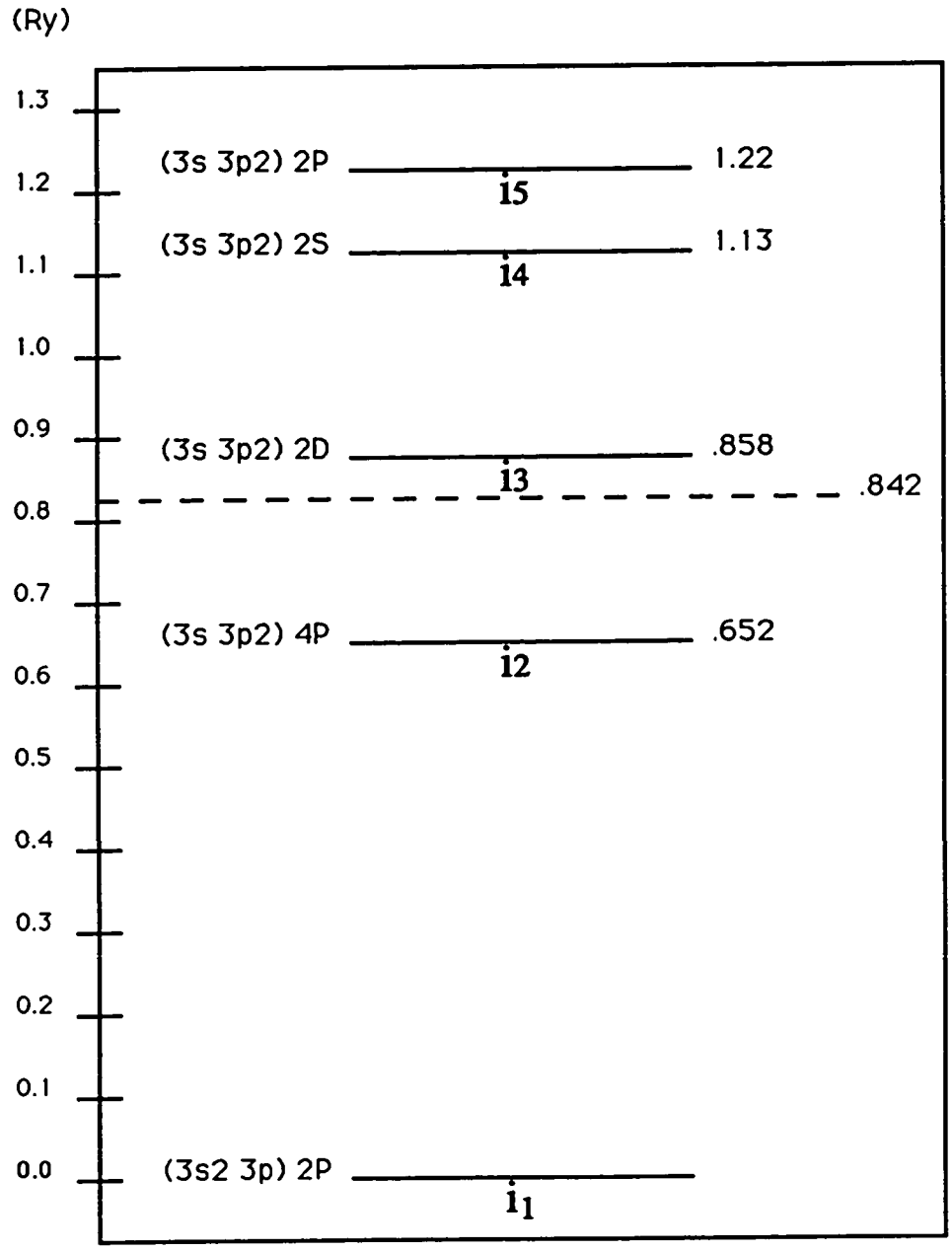

Figure 4.1. The energy level diagram of S^{3+}.

Table 4.1. Values of $\bar{\sigma}^{DR}(cm^2)$ and $\bar{\sigma}^{RES}(cm^2)$ as functions of e_c(Ry) for the transitions $i_1 \rightarrow d_1$, and $i_1 \rightarrow d_1 \rightarrow i_1$, respectively. Δe_c = 0.01 Ry. Powers of 10 are shown in parenthesis.

	$i_1 \rightarrow d_1$	
e_c	DR	i_1
0.06	1.96(-19)	1.95(-16)
0.10	1.73(-20)	2.43(-15)
0.23	2.96(-21)	7.86(-16)
0.25	4.71(-21)	5.05(-16)
0.28	2.87(-20)	3.86(-17)
0.30	3.33(-21)	3.76(-16)
0.37	5.28(-22)	2.58(-16)
0.38	1.87(-21)	1.75(-16)
0.39	1.23(-20)	1.97(-17)
0.40	1.51(-21)	1.49(-16)
0.44	4.41(-25)	1.24(-16)
0.45	1.05(-21)	8.61(-17)
0.46	6.72(-21)	1.18(-17)
0.47	8.72(-22)	7.82(-17)
0.49	2.67(-25)	7.08(-17)
0.50	4.77(-21)	5.89(-17)
0.51	1.03(-21)	8.21(-17)
0.52	3.94(-22)	3.28(-17)
0.53	3.07(-21)	7.58(-17)
0.54	5.45(-22)	7.47(-17)
0.55	2.49(-21)	7.16(-17)
0.56	1.93(-21)	4.51(-17)
0.57	1.38(-21)	4.47(-17)
0.58	1.24(-21)	5.88(-17)
0.59	1.07(-21)	5.03(-17)
0.60	1.60(-21)	4.18(-17)
0.61	8.67(-22)	2.56(-17)
0.62	9.70(-22)	1.71(-17)
0.63	9.54(-22)	7.53(-18)
0.64	6.49(-23)	1.27(-19)
Total	3.01(-19)	5.99(-15)

Table 4.2. Values of $\bar{\sigma}^{DR}(cm^2)$ and $\bar{\sigma}^{RE}(cm^2)$ as functions of e_c(Ry) for the transitions $i_1 \rightarrow d_2$, and $i_1 \rightarrow d_2 \rightarrow i_1, d_1$, respectively.

	$i_1 \rightarrow d_2$		
e_c	DR	i_1	d_1
0.17	2.91(-19)	8.86(-15)	
0.21	7.21(-20)	2.69(-15)	
0.27	4.18(-19)	1.21(-14)	
0.30	8.56(-20)	4.93(-15)	
0.44	8.62(-20)	1.36(-15)	
0.46	2.40(-20)	5.86(-16)	
0.48	1.75(-19)	3.72(-15)	
0.49	1.08(-19)	8.10(-16)	
0.50	4.88(-20)	1.45(-15)	
0.57	6.64(-20)	5.15(-16)	
0.58	1.61(-20)	2.51(-16)	
0.60	3.22(-19)	2.36(-15)	
0.61	3.91(-20)	6.77(-16)	
0.65	3.83(-20)	2.15(-16)	5.42(-17)
0.66	8.95(-21)	1.24(-16)	1.20(-17)
0.67	4.05(-19)	1.72(-15)	9.41(-17)
0.70	3.72(-20)	2.02(-16)	3.87(-17)
0.71	4.44(-19)	9.13(-16)	2.76(-17)
0.72	2.00(-20)	2.14(-16)	3.23(-17)
0.73	3.56(-20)	1.35(-16)	2.52(-17)
0.74	5.58(-19)	8.26(-16)	4.57(-17)
0.75	6.06(-20)	2.22(-16)	3.61(-17)
0.76	5.50(-19)	6.18(-16)	3.79(-17)
0.77	5.83(-20)	1.21(-16)	2.09(-17)
0.78	5.96(-19)	4.96(-16)	3.86(-17)
0.79	1.07(-18)	5.84(-16)	3.45(-17)
0.80	1.36(-18)	4.18(-16)	3.17(-17)
0.81	2.43(-18)	3.34(-16)	2.60(-17)
0.82	4.47(-18)	2.52(-16)	1.45(-17)
0.83	5.15(-18)	2.49(-16)	1.37(-17)
0.84	2.07(-17)	1.48(-16)	4.63(-18)
Total	3.97(-17)	4.81(-14)	5.88(-16)

Table 4.3. Values of $\bar{\sigma}^{DR}(cm^2)$ and $\bar{\sigma}^{RE}(cm^2)$ as functions of e_c(Ry) for the transitions $d_1 \rightarrow d_2$, and $d_1 \rightarrow d_2 \rightarrow i_1, d_1$, respectively.

	$d_1 \rightarrow d_2$		
e_c	DR	i_1	d_1
0.01	1.60(-19)	7.44(-16)	2.52(-16)
0.02	1.41(-19)	6.79(-16)	1.14(-15)
0.05	8.57(-20)	2.58(-16)	6.27(-16)
0.06	9.25(-20)	3.27(-16)	3.32(-16)
0.07	2.68(-21)	2.43(-17)	2.32(-18)
0.08	7.56(-20)	1.81(-16)	4.00(-16)
0.09	4.20(-20)	9.12(-17)	2.81(-17)
0.10	6.57(-20)	1.29(-16)	2.44(-16)
0.11	7.38(-20)	1.28(-16)	1.35(-16)
0.12	7.21(-20)	8.03(-17)	1.61(-16)
0.13	1.25(-19)	1.03(-16)	1.68(-16)
0.14	1.92(-19)	1.09(-16)	1.32(-16)
0.15	5.07(-19)	6.98(-17)	1.09(-16)
0.16	2.97(-18)	5.45(-17)	8.70(-17)
0.17	3.45(-19)	2.98(-17)	5.17(-17)
0.18	3.66(-18)	2.55(-17)	3.58(-17)
0.19	1.27(-18)	5.78(-18)	1.96(-18)
Total	9.87(-18)	3.04(-15)	3.91(-15)

Table 4.4. Values of $\bar{\sigma}^{DR}(cm^2)$ and $\bar{\sigma}^{RE}(cm^2)$ as functions of e_c(Ry) for the transitions $i_1 \rightarrow d_3$, and $i_1 \rightarrow d_3 \rightarrow i_1, d_1, d_2$, respectively.

	$i_1 \rightarrow d_3$			
e_c	DR	i_1	d_1	d_2
0.44	3.47(-20)	7.17(-16)		
0.48	9.54(-21)	2.38(-16)		
0.54	5.70(-20)	1.07(-15)		
0.58	4.89(-21)	5.32(-16)		
0.71	1.40(-20)	1.03(-16)	6.34(-17)	
0.73	4.84(-21)	7.36(-17)		
0.76	6.48(-20)	5.88(-16)	1.86(-17)	
0.77	9.72(-21)	1.60(-16)	3.07(-17)	
0.84	1.23(-20)	4.82(-17)	2.29(-17)	
0.85	2.00(-21)	2.41(-17)		1.02(-17)
0.87	3.12(-20)	1.90(-16)	6.74(-18)	1.27(-16)
0.88	1.58(-20)	5.60(-17)	1.01(-17)	3.73(-17)
0.92	3.96(-21)	1.35(-17)	6.29(-18)	1.88(-17)
0.93	1.55(-21)	1.35(-17)		5.80(-18)
0.94	5.68(-20)	1.17(-16)	4.04(-18)	8.41(-17)
0.95	4.38(-21)	3.20(-17)	5.80(-18)	1.81(-17)
0.97	3.67(-21)	7.81(-18)	3.59(-18)	1.14(-17)
0.98	7.79(-20)	8.90(-17)	2.75(-18)	5.82(-17)
0.99	4.24(-21)	2.06(-17)	3.66(-18)	1.15(-17)
1.00	1.45(-21)	6.10(-18)		2.60(-18)
1.01	2.04(-20)	6.16(-17)	6.73(-18)	4.08(-17)
1.02	8.79(-20)	1.89(-17)	1.39(-20)	1.49(-17)
1.03	2.28(-20)	4.94(-17)	4.87(-18)	3.15(-17)
1.04	1.03(-19)	3.92(-17)	4.72(-18)	2.70(-17)
1.05	1.09(-19)	4.18(-17)	3.05(-18)	2.80(-17)
1.06	2.09(-19)	5.72(-17)	4.09(-18)	4.00(-17)
1.07	1.59(-19)	3.44(-17)	2.85(-18)	2.28(-17)
1.08	4.88(-19)	3.31(-17)	2.76(-18)	2.30(-17)
1.09	9.77(-18)	2.63(-17)	2.13(-18)	1.92(-17)
1.10	6.61(-19)	2.45(-17)	1.50(-18)	1.82(-17)
1.11	3.91(-18)	2.00(-17)	7.79(-19)	1.39(-17)
1.12	9.74(-19)	1.46(-19)	6.02(-23)	1.18(-19)
Total	8.14(-18)	4.50(-15)	2.12(-16)	6.64(-16)

Table 4.5. Values of $\bar{\sigma}^{DR}(cm^2)$ and $\bar{\sigma}^{RE}(cm^2)$ as functions of e_c(Ry) for the transitions $d_1 \rightarrow d_3$, and $d_1 \rightarrow d_3 \rightarrow i_1, d_1, d_2$, respectively.

	$d_1 \rightarrow d_3$			
e_c	DR	i_1	d_1	d_2
0.06	3.34(-20)	3.76(-16)	2.34(-16)	
0.10	4.35(-21)	6.54(-17)	3.27(-18)	
0.11	4.67(-23)	1.56(-19)	9.09(-23)	
0.12	4.29(-21)	9.49(-17)	1.93(-17)	
0.19	8.60(-21)	4.96(-17)	2.38(-17)	
0.22	1.37(-21)	1.33(-17)	7.46(-19)	7.87(-18)
0.23	1.52(-21)	1.92(-17)	3.75(-18)	1.02(-17)
0.27	3.08(-21)	1.06(-17)	4.94(-18)	1.46(-17)
0.29	2.14(-21)	1.58(-17)	2.10(-18)	8.88(-18)
0.32	2.52(-21)	5.41(-18)	2.49(-18)	7.84(-18)
0.33	8.20(-22)	4.05(-18)	2.46(-19)	2.37(-18)
0.34	9.85(-22)	5.34(-18)	9.69(-19)	2.66(-18)
0.35	2.19(-21)	3.14(-18)	1.40(-18)	4.69(-18)
0.36	1.70(-21)	6.32(-18)	8.30(-19)	3.38(-18)
0.37	2.96(-21)	4.80(-18)	1.45(-18)	4.55(-18)
0.38	2.43(-21)	5.32(-18)	7.46(-19)	2.81(-18)
0.39	2.81(-21)	2.75(-18)	9.12(-19)	2.92(-18)
0.40	6.12(-21)	5.11(-18)	1.31(-18)	4.72(-18)
0.41	8.17(-21)	5.03(-18)	1.04(-18)	3.93(-18)
0.42	1.03(-20)	3.52(-18)	7.33(-19)	2.69(-18)
0.43	3.84(-20)	3.62(-18)	8.07(-19)	2.90(-18)
0.44	1.31(-19)	2.08(-18)	5.32(-19)	2.08(-18)
0.45	2.44(-19)	1.63(-18)	4.32(-19)	1.74(-18)
0.46	9.03(-20)	5.34(-19)	3.31(-20)	3.13(-19)
Total	6.03(-19)	7.04(-16)	3.05(-16)	9.11(-17)

Table 4.6. Values of $\bar{\sigma}^{DR}(cm^2)$ and $\bar{\sigma}^{RE}(cm^2)$ as functions of e_c(Ry) for the transitions $d_2 \rightarrow d_3$, and $d_2 \rightarrow d_3 \rightarrow i_1, d_1, d_2$. respectively.

	$d_2 \rightarrow d_3$			
e_c	DR	i_1	d_1	d_2
0.01	3.24(-19)	3.04(-15)	1.30(-16)	1.92(-15)
0.02	9.72(-19)	1.63(-15)	1.03(-16)	1.54(-15)
0.06	7.32(-20)	1.51(-16)	6.98(-17)	3.81(-15)
0.07	1.03(-20)	4.28(-17)		3.85(-17)
0.08	4.00(-19)	5.56(-16)	1.72(-17)	4.20(-16)
0.09	2.24(-20)	1.12(-16)	1.83(-17)	9.28(-17)
0.11	4.35(-20)	5.66(-17)	2.58(-17)	1.35(-16)
0.12	4.00(-20)	1.75(-16)	7.33(-18)	1.15(-16)
0.13	3.25(-19)	1.42(-16)	8.16(-18)	1.19(-16)
0.14	5.44(-21)	1.09(-17)		9.78(-18)
0.15	7.47(-20)	1.51(-16)	2.26(-17)	1.56(-16)
0.16	3.30(-19)	6.39(-17)	3.73(-20)	5.24(-17)
0.17	5.50(-20)	5.33(-17)	1.20(-17)	7.57(-17)
0.18	3.78(-19)	1.48(-16)	1.44(-17)	1.32(-16)
0.19	3.06(-19)	7.59(-17)	3.05(-18)	5.48(-17)
0.20	4.24(-19)	1.25(-16)	1.46(-17)	1.27(-16)
0.21	6.13(-19)	5.97(-17)	6.28(-18)	5.98(-17)
0.22	1.13(-18)	7.28(-17)	6.79(-18)	6.49(-17)
0.23	2.07(-18)	5.22(-17)	5.11(-18)	5.04(-17)
0.24	1.76(-18)	4.74(-17)	4.29(-18)	4.58(-17)
0.25	6.68(-18)	3.96(-17)	2.00(-18)	3.11(-17)
0.26	4.74(-18)	2.18(-18)	3.40(-20)	1.60(-18)
Total	2.08(-17)	6.81(-15)	4.71(-16)	5.59(-15)

Table 4.7. Values of $\bar{\sigma}^{DR}(cm^2)$ and $\bar{\sigma}^{RE}(cm^2)$ as functions of e_c(Ry) for the transitions $i_1 \rightarrow d_4$, and $i_1 \rightarrow d_4 \rightarrow i_1, d_1, d_2, d_3$, respectively.

	$i_1 \rightarrow d_4$				
e_c	DR	i_1	d_1	d_2	d_3
0.53	3.40(-19)	4.31(-15)			
0.57	7.82(-20)	1.28(-15)			
0.63	5.12(-19)	9.51(-15)			
0.67	1.55(-19)	3.66(-15)	2.61(-17)		
0.80	1.96(-19)	1.06(-15)	2.82(-17)		
0.82	4.71(-20)	4.17(-16)	1.63(-17)		
0.85	6.53(-19)	4.69(-15)	1.94(-17)	1.34(-19)	
0.86	1.10(-19)	1.27(-15)	7.20(-18)	1.08(-16)	
0.93	1.83(-19)	3.80(-16)	1.07(-17)	7.60(-17)	
0.94	3.86(-20)	1.94(-16)	7.34(-18)	7.67(-18)	
0.96	5.53(-19)	2.53(-15)	1.07(-17)	3.33(-17)	
0.97	4.00(-19)	7.00(-16)	3.23(-18)	6.32(-17)	
1.01	8.59(-20)	1.55(-16)	3.22(-18)	3.84(-17)	
1.02	2.92(-20)	1.12(-16)	4.05(-18)	4.31(-18)	
1.03	1.22(-18)	1.64(-15)	6.53(-18)	1.73(-17)	
1.04	7.60(-20)	3.85(-16)	1.77(-18)	3.60(-17)	
1.06	1.15(-19)	1.27(-16)	3.41(-18)	2.33(-17)	
1.07	2.21(-19)	8.07(-16)	6.73(-18)	1.47(-17)	
1.08	1.28(-18)	6.18(-16)	1.15(-18)	2.27(-17)	9.47(-21)
1.09	2.74(-20)	5.14(-17)	1.79(-18)	1.92(-18)	
1.10	3.99(-19)	7.99(-16)	7.27(-18)	3.95(-17)	6.79(-21)
1.11	1.50(-18)	2.77(-16)	4.62(-20)	5.42(-20)	
1.12	4.45(-19)	6.20(-16)	6.70(-18)	3.03(-17)	5.03(-21)
1.13	1.79(-18)	5.04(-16)	3.16(-18)	3.04(-17)	5.13(-18)
1.14	1.87(-18)	5.52(-16)	3.54(-18)	1.75(-17)	2.79(-18)
1.15	3.51(-18)	7.12(-16)	4.95(-18)	2.35(-17)	3.91(-18)
1.16	2.71(-18)	4.24(-16)	3.46(-18)	1.68(-17)	2.56(-18)
1.17	6.92(-18)	4.04(-16)	2.35(-18)	1.60(-17)	2.43(-18)
1.18	1.33(-17)	3.37(-16)	2.15(-18)	1.18(-17)	2.13(-18)
1.19	1.04(-17)	3.02(-16)	1.81(-18)	7.70(-18)	1.62(-18)
1.20	4.54(-17)	2.43(-16)	9.77(-19)	2.92(-18)	6.06(-19)
1.21	8.53(-18)	1.31(-18)	1.82(-22)	1.90(-22)	1.44(-23)
Total	1.03(-16)	3.91(-14)	1.94(-16)	6.43(-16)	2.12(-17)

Table 4.8. Values of $\bar{\sigma}^{DR}(cm^2)$ and $\bar{\sigma}^{RE}(cm^2)$ as functions of e_c(Ry) for the transitions $d_1 \rightarrow d_4$, and $d_1 \rightarrow d_4 \rightarrow i_1$, d_1, d_2, d_3, respectively.

	$d_1 \rightarrow d_4$				
e_c	DR	i_1	d_1	d_2	d_3
0.01	2.94(-19)	4.86(-16)	1.55(-15)		
0.15	8.51(-20)	7.54(-17)	1.06(-16)		
0.17	6.14(-21)	3.94(-17)	2.91(-18)		
0.19	1.33(-20)	4.15(-17)	9.89(-19)		
0.20	1.95(-23)	6.84(-20)	4.06(-24)	3.65(-24)	
0.21	2.39(-20)	1.45(-17)	5.77(-17)	7.25(-19)	
0.28	3.82(-20)	1.75(-17)	2.01(-17)	4.68(-18)	
0.29	3.15(-21)	1.17(-17)	8.06(-19)	2.06(-19)	
0.31	9.59(-21)	1.65(-17)	4.47(-19)	2.28(-19)	
0.32	1.58(-20)	4.86(-18)	2.08(-17)	2.27(-19)	
0.36	6.75(-20)	4.49(-18)	1.06(-17)	2.95(-18)	
0.37	1.95(-21)	5.57(-18)	3.62(-19)	9.47(-20)	
0.38	2.01(-20)	1.12(-17)	1.07(-17)	2.25(-19)	
0.41	2.00(-20)	7.59(-18)	4.63(-18)	1.06(-18)	
0.42	6.47(-21)	5.41(-18)	1.68(-19)	7.65(-20)	
0.43	9.87(-21)	1.37(-18)	6.19(-18)	5.84(-20)	
0.44	1.79(-20)	4.98(-18)	2.76(-18)	6.35(-19)	
0.45	1.62(-20)	6.17(-18)	4.51(-18)	1.12(-19)	
0.46	2.76(-20)	4.75(-18)	5.08(-18)	4.81(-19)	
0.47	2.39(-20)	4.16(-18)	4.28(-18)	8.25(-20)	9.24(-21)
0.48	2.77(-20)	3.14(-18)	2.83(-18)	3.39(-19)	3.84(-20)
0.49	5.46(-20)	4.95(-18)	3.94(-18)	4.57(-19)	3.60(-20)
0.50	6.84(-20)	4.78(-18)	3.19(-18)	2.15(-19)	1.84(-20)
0.51	1.80(-19)	4.22(-18)	3.23(-18)	3.31(-19)	2.56(-20)
0.52	3.91(-19)	2.78(-18)	2.67(-18)	2.35(-19)	2.00(-20)
0.53	4.19(-19)	1.91(-18)	9.30(-19)	1.89(-19)	1.43(-20)
0.54	6.84(-19)	1.93(-18)	6.40(-19)	1.53(-19)	1.26(-20)
0.55	2.33(-19)	6.75(-19)	2.04(-20)	6.42(-21)	9.88(-22)
Total	2.76(-18)	7.88(-16)	1.83(-15)	1.38(-17)	1.75(-19)

Table 4.9. Values of $\overline{\sigma}^{DR}(cm^2)$ and $\overline{\sigma}^{RE}(cm^2)$ as functions of e_c(Ry) for the transitions $d_2 \rightarrow d_4$, and $d_2 \rightarrow d_4 \rightarrow i_1$, d_1, d_2, d_3, respectively.

	$d_2 \rightarrow d_4$				
e_c	DR	i_1	d_1	d_2	d_3
0.08	2.17(-19)	5.35(-16)	2.01(-17)	2.91(-16)	
0.09	7.24(-21)	4.80(-17)	8.06(-19)	2.61(-18)	
0.10	6.66(-20)	1.81(-16)	8.04(-19)	1.53(-17)	
0.11	4.99(-20)	3.15(-16)	7.50(-19)	5.71(-17)	
0.15	1.46(-19)	1.47(-16)	8.13(-18)	7.64(-17)	
0.16	3.16(-21)	1.60(-17)	2.55(-19)	8.57(-19)	
0.17	5.60(-20)	6.12(-17)	3.17(-19)	6.22(-18)	
0.18	2.08(-20)	1.23(-16)	2.66(-19)	2.13(-17)	
0.20	6.71(-20)	7.18(-17)	2.41(-18)	3.44(-17)	
0.21	3.71(-20)	4.36(-17)	3.02(-19)	1.01(-17)	
0.22	4.30(-20)	6.59(-17)	1.35(-19)	1.10(-17)	7.22(-21)
0.23	2.19(-21)	5.38(-18)	8.23(-20)	2.82(-19)	
0.24	1.01(-19)	1.03(-16)	1.52(-18)	3.27(-17)	4.83(-21)
0.25	1.14(-20)	3.92(-18)	5.78(-20)	2.00(-19)	
0.26	7.22(-20)	6.51(-17)	1.06(-18)	1.84(-17)	3.40(-21)
0.27	1.26(-19)	8.63(-17)	8.41(-19)	2.21(-17)	1.60(-18)
0.28	4.93(-20)	2.15(-17)	1.03(-19)	4.74(-18)	2.26(-19)
0.29	2.38(-19)	6.83(-17)	1.24(-18)	2.33(-17)	9.63(-19)
0.30	2.03(-19)	3.69(-17)	4.94(-19)	1.03(-17)	5.79(-19)
0.31	5.60(-19)	3.87(-17)	4.68(-19)	1.11(-17)	5.74(-19)
0.32	1.80(-18)	2.47(-17)	4.11(-19)	8.37(-18)	3.62(-19)
0.33	1.00(-18)	1.65(-17)	3.60(-19)	7.01(-18)	1.69(-19)
0.34	3.18(-18)	7.65(-18)	7.94(-20)	2.73(-18)	4.49(-20)
0.35	3.96(-19)	1.49(-19)	1.61(-22)	1.99(-20)	3.03(-23)
Total	8.45(-18)	2.09(-15)	4.09(-17)	6.68(-16)	4.54(-18)

Table 4.10. Values of $\bar{\sigma}^{DR}(cm^2)$ and $\bar{\sigma}^{RE}(cm^2)$ as functions of e_c(Ry) for the transitions $d_3 \rightarrow d_4$, and $d_3 \rightarrow d_4 \rightarrow i_1$, d_1, d_2, d_3, respectively.

	$d_3 \rightarrow d_4$				
e_c	DR	i_1	d_1	d_2	d_3
0.01	1.46(-18)	1.08(-15)	6.78(-18)	1.24(-16)	8.51(-17)
0.02	5.46(-19)	2.80(-16)	1.57(-18)	2.26(-17)	1.88(-17)
0.03	7.06(-19)	2.08(-16)	1.45(-18)	1.96(-17)	1.85(-17)
0.04	1.07(-18)	1.74(-16)	1.30(-18)	1.76(-17)	1.70(-17)
0.05	2.09(-18)	1.44(-16)	9.73(-19)	1.42(-17)	1.25(-17)
0.06	9.49(-18)	8.91(-17)	6.70(-19)	6.38(-18)	9.14(-18)
0.07	8.35(-18)	1.96(-17)	7.42(-20)	2.74(-19)	8.54(-19)
Total	2.37(-17)	1.99(-15)	1.28(-17)	2.05(-16)	1.62(-16)

Table 4.11. Values of $\bar{\sigma}^{DR}(cm^2)$ and $\bar{\sigma}^{RE}(cm^2)$ as functions of ℓ for the transitions $i_1 \rightarrow d_1$, and $i_1 \rightarrow d_1 \rightarrow i_1$, respectively.

	$i_1 \rightarrow d_1$	
ℓ	DR	i_1
0	1.07(-20)	9.97(-16)
1	2.56(-20)	3.25(-15)
2	3.49(-21)	1.44(-15)
3	2.61(-19)	2.99(-16)
Total	3.01(-19)	5.99(-15)

Table 4.12. Values of $\bar{\sigma}^{DR}(cm^2)$ and $\bar{\sigma}^{RE}(cm^2)$ as functions of ℓ for the transitions $i_1 \rightarrow d_2$, and $i_1 \rightarrow d_2 \rightarrow i_1, d_1$, respectively.

	$i_1 \rightarrow d_2$		
ℓ	DR	i_1	d_1
0	1.43(-18)	4.01(-15)	4.64(-17)
1	3.84(-18)	8.39(-15)	2.03(-16)
2	3.69(-18)	1.15(-14)	1.80(-16)
3	9.47(-18)	2.11(-14)	1.58(-16)
4	7.38(-18)	2.70(-15)	1.25(-18)
5	5.41(-18)	3.77(-16)	1.00(-19)
6	3.36(-18)	6.89(-17)	1.98(-20)
7	2.77(-18)	2.99(-17)	5.95(-21)
8	2.49(-18)	1.66(-17)	2.26(-21)
Total	3.98(-17)	4.81(-14)	5.88(-16)

Table 4.13. Values of $\bar{\sigma}^{DR}(cm^2)$ and $\bar{\sigma}^{RE}(cm^2)$ as functions of ℓ for the transitions $d_1 \rightarrow d_2$, and $d_1 \rightarrow d_2 \rightarrow i_1$, d_1, respectively.

	$d_1 \rightarrow d_2$		
ℓ	DR	i_1	d_1
0	3.05(-19)	1.39(-16)	1.32(-17)
1	3.29(-18)	1.22(-15)	2.04(-15)
2	4.19(-18)	5.06(-16)	1.46(-15)
3	1.83(-18)	1.16(-15)	3.99(-16)
4	1.15(-19)	8.07(-18)	2.42(-19)
5	5.50(-20)	7.50(-19)	2.78(-20)
6	4.18(-20)	1.60(-19)	5.83(-21)
7	2.22(-20)	2.44(-20)	1.25(-21)
8	1.45(-20)	7.34(-21)	3.89(-22)
Total	9.87(-18)	3.04(-15)	3.91(-15)

Table 4.14. Values of $\bar{\sigma}^{DR}(cm^2)$ and $\bar{\sigma}^{RE}(cm^2)$ as functions of ℓ for the transitions $i_1 \rightarrow d_3$, and $i_1 \rightarrow d_3 \rightarrow i_1, d_1, d_2$, respectively.

	$i_1 \rightarrow d_3$			
ℓ	DR	i_1	d_1	d_2
0	2.89(-19)	3.90(-16)		3.34(-17)
1	8.01(-19)	8.76(-16)	6.42(-17)	1.04(-16)
2	5.84(-19)	9.13(-16)	1.07(-16)	6.59(-17)
3	1.95(-18)	2.02(-15)	4.11(-17)	2.95(-16)
4	1.77(-18)	2.77(-16)	1.79(-19)	1.26(-16)
5	1.01(-18)	2.44(-17)	1.76(-22)	3.04(-17)
6	6.56(-19)	4.88(-18)	3.64(-23)	5.47(-18)
7	5.62(-19)	2.20(-18)	1.97(-23)	2.34(-18)
8	5.14(-19)	1.24(-18)	1.13(-23)	1.30(-18)
Total	8.14(-18)	4.50(-15)	2.12(-16)	6.64(-16)

Table 4.15. Values of $\overline{\sigma}^{DR}(cm^2)$ and $\overline{\sigma}^{RE}(cm^2)$ as functions of ℓ for the transitions $d_1 \rightarrow d_3$, and $d_1 \rightarrow d_3 \rightarrow i_1$, d_1, d_2, respectively.

	$d_1 \rightarrow d_3$			
ℓ	DR	i_1	d_1	d_2
1	1.64(-19)	1.47(-16)	2.91(-17)	2.66(-17)
2	3.24(-19)	4.55(-16)	2.71(-16)	4.32(-17)
3	1.13(-19)	1.01(-16)	5.38(-18)	2.12(-17)
4	1.88(-21)	3.54(-19)	3.07(-22)	1.47(-19)
5	6.38(-24)	2.42(-22)	2.08(-27)	2.83(-22)
6	4.62(-24)	4.87(-23)	4.54(-28)	5.11(-23)
7	4.25(-24)	2.65(-23)	2.56(-28)	2.83(-23)
8	4.09(-24)	1.48(-23)	1.38(-28)	1.54(-23)
Total	6.03(-19)	7.04(-16)	3.05(-16)	9.11(-17)

Table 4.16. Values of $\bar{\sigma}^{DR}(cm^2)$ and $\bar{\sigma}^{RE}(cm^2)$ as functions of ℓ for the transitions $d_2 \rightarrow d_3$, and $d_2 \rightarrow d_3 \rightarrow i_1$, d_1, d_2, respectively.

	$d_2 \rightarrow d_3$			
ℓ	DR	i_1	d_1	d_2
0	5.89(-19)	1.08(-16)		9.69(-17)
1	1.67(-18)	8.95(-16)	1.51(-16)	7.44(-16)
2	3.17(-18)	3.24(-16)	1.47(-16)	7.73(-16)
3	3.35(-18)	3.93(-15)	1.71(-16)	2.50(-15)
4	3.54(-18)	1.27(-15)	8.81(-19)	1.00(-15)
5	3.36(-18)	2.50(-16)	1.27(-21)	4.34(-16)
6	1.96(-18)	2.28(-17)	1.34(-22)	2.74(-17)
7	1.63(-18)	8.22(-18)	7.47(-23)	8.83(-18)
8	1.49(-18)	4.15(-18)	3.87(-23)	4.33(-18)
Total	2.08(-17)	6.81(-15)	4.71(-16)	5.59(-15)

Table 4.17. Values of $\overline{\sigma}^{DR}(cm^2)$ and $\overline{\sigma}^{RE}(cm^2)$ as functions of ℓ for the transitions $i_1 \rightarrow d_4$, and $i_1 \rightarrow d_4 \rightarrow i_1, d_1, d_2, d_3$, respectively.

	$i_1 \rightarrow d_4$				
ℓ	DR	i_1	d_1	d_2	d_3
0	3.73(-18)	2.34(-15)	3.96(-17)	2.48(-17)	
1	1.07(-17)	7.14(-15)	4.35(-17)	3.14(-16)	6.01(-18)
2	1.03(-17)	6.41(-15)	5.59(-17)	2.09(-16)	1.08(-17)
3	2.41(-17)	1.95(-14)	5.47(-17)	9.48(-17)	4.35(-18)
4	1.95(-17)	3.09(-15)	4.76(-19)	6.61(-19)	1.59(-20)
5	1.37(-17)	4.35(-16)	3.87(-21)	4.16(-20)	
6	8.35(-18)	8.09(-17)	6.48(-22)	7.67(-21)	
7	6.81(-18)	3.43(-17)	2.06(-22)	3.47(-21)	
8	6.02(-18)	1.86(-17)	8.34(-23)	1.86(-21)	
Total	1.03(-16)	3.91(-14)	1.94(-16)	6.43(-16)	2.12(-17)

Table 4.18. Values of $\overline{\sigma}^{DR}(cm^2)$ and $\overline{\sigma}^{RE}(cm^2)$ as functions of ℓ for the transitions $d_1 \rightarrow d_4$, and $d_1 \rightarrow d_4 \rightarrow i_1$, d_1, d_2, d_3, respectively.

	$d_1 \rightarrow d_4$				
ℓ	DR	i_1	d_1	d_2	d_3
0	1.82(-19)	7.11(-17)	4.97(-18)	5.35(-19)	
1	1.05(-18)	5.14(-16)	1.67(-15)	1.32(-18)	3.16(-20)
2	1.13(-18)	1.14(-16)	1.52(-16)	1.13(-17)	1.29(-19)
3	3.86(-19)	8.83(-17)	2.46(-18)	6.45(-19)	1.48(-20)
4	6.31(-21)	6.37(-19)	3.40(-22)	9.57(-23)	
5	8.60(-22)	4.89(-21)	1.73(-23)	2.08(-24)	
6	5.73(-22)	8.14(-22)	2.31(-24)	2.68(-25)	
7	2.20(-22)	2.48(-22)	3.95(-25)	1.05(-25)	
8	2.67(-23)	9.71(-23)	6.11(-28)	3.93(-27)	
Total	2.76(-18)	7.88(-16)	1.83(-15)	1.38(-17)	1.75(-19)

Table 4.19. Values of $\bar{\sigma}^{DR}(cm^2)$ and $\bar{\sigma}^{RE}(cm^2)$ as functions of ℓ for the transitions $d_2 \rightarrow d_4$, and $d_2 \rightarrow d_4 \rightarrow i_1$, d_1, d_2, d_3, respectively.

	$d_2 \rightarrow d_4$				
ℓ	DR	i_1	d_1	d_2	d_3
0	2.55(-19)	9.74(-17)	1.57(-18)	5.22(-18)	
1	1.91(-18)	7.08(-16)	1.57(-18)	1.23(-16)	2.79(-18)
2	4.33(-18)	9.24(-16)	3.61(-17)	4.83(-16)	1.73(-18)
3	1.82(-18)	3.54(-16)	1.75(-18)	5.63(-17)	1.09(-20)
4	1.08(-19)	1.82(-18)	2.98(-22)	3.60(-20)	
5	1.08(-20)	1.22(-19)	4.82(-24)	1.76(-22)	
6	5.10(-21)	2.03(-20)	6.20(-25)	2.15(-23)	
7	3.72(-21)	8.76(-21)	2.43(-25)	8.03(-24)	
8	2.72(-21)	4.47(-21)	8.28(-27)	3.27(-24)	
Total	8.45(-18)	2.09(-15)	4.09(-17)	6.68(-16)	4.53(-18)

Table 4.20. Values of $\bar{\sigma}^{DR}(cm^2)$ and $\bar{\sigma}^{RE}(cm^2)$ as functions of ℓ for the transitions $d_3 \rightarrow d_4$, and $d_3 \rightarrow d_4 \rightarrow i_1$, d_1, d_2, d_3, respectively.

	$d_3 \rightarrow d_4$				
ℓ	DR	i_1	d_1	d_2	d_3
1	5.67(-18)	7.61(-16)	3.51(-18)	3.51(-18)	4.56(-17)
2	1.48(-17)	7.42(-16)	7.83(-18)	7.83(-18)	1.07(-16)
3	3.22(-18)	4.85(-16)	1.48(-18)	1.48(-18)	9.60(-18)
4	2.02(-20)	2.00(-18)			7.44(-22)
Total	2.37(-17)	1.99(-15)	1.28(-17)	2.05(-16)	1.62(-16)

Table 4.21. The rate coefficients $\overline{\alpha}^{DR}(cm^3/sec)$ and $\overline{\alpha}^{RES}(cm^3/sec)$ as functions of kT(Ry) for the transitions $i_1 \rightarrow d_1$, and $i_1 \rightarrow d_1 \rightarrow i_1$, respectively.

	$i_1 \rightarrow d_1$	
kT(Ry)	DR	i_1
1.0(-03)	0.38(-34)	0.12(-29)
2.0(-03)	0.63(-24)	0.63(-21)
4.0(-03)	0.54(-17)	0.54(-14)
6.0(-03)	0.85(-15)	0.90(-12)
8.0(-03)	0.94(-14)	0.12(-10)
1.0(-02)	0.37(-13)	0.59(-10)
3.0(-02)	0.68(-12)	0.46(-08)
5.0(-02)	0.82(-12)	0.85(-08)
8.0(-02)	0.72(-12)	0.10(-07)
1.0(-01)	0.65(-12)	0.11(-07)
3.0(-01)	0.31(-12)	0.80(-08)
5.0(-01)	0.19(-12)	0.54(-08)
8.0(-01)	0.12(-12)	0.34(-08)
1.0(-00)	0.90(-13)	0.26(-08)
3.0(-00)	0.21(-13)	0.63(-09)
5.0(-00)	0.10(-13)	0.31(-09)
8.0(-00)	0.51(-14)	0.15(-09)
1.0(+01)	0.37(-14)	0.11(-09)
1.2(+01)	0.28(-14)	0.86(-10)
1.5(+01)	0.20(-14)	0.62(-10)

Table 4.22. The rate coefficients $\bar{\alpha}^{DR}(cm^3/sec)$ and $\bar{\alpha}^{RE}(cm^3/sec)$ as functions of kT(Ry) for the transitions $i_1 \rightarrow d_2$, and $i_1 \rightarrow d_2 \rightarrow i_1, d_1$, respectively.

	$i_1 \rightarrow d_2$		
kT(Ry)	DR	i_1	d_1
1.0(-03)	0.23(-11)	1.5(-29)	3.4(-31)
2.0(-03)	0.16(-10)	5.2(-30)	1.2(-31)
4.0(-03)	0.25(-10)	1.9(-24)	4.2(-32)
6.0(-03)	0.32(-10)	2.1(-18)	2.3(-32)
8.0(-03)	0.40(-10)	1.9(-15)	1.5(-32)
1.0(-02)	0.43(-10)	1.1(-13)	1.1(-32)
3.0(-02)	0.43(-10)	2.6(-09)	1.4(-17)
5.0(-02)	0.40(-10)	1.6(-08)	5.9(-14)
8.0(-02)	0.35(-10)	4.0(-08)	5.5(-12)
1.0(-01)	0.30(-10)	5.2(-08)	2.3(-11)
3.0(-01)	0.24(-10)	6.9(-08)	5.6(-10)
5.0(-01)	0.19(-10)	5.3(-08)	6.9(-10)
8.0(-01)	0.15(-10)	3.6(-08)	5.9(-10)
1.0(-00)	0.11(-10)	2.9(-08)	5.1(-10)
3.0(-00)	0.84(-11)	7.6(-09)	1.6(-10)
5.0(-00)	0.61(-11)	3.8(-09)	8.3(-11)
8.0(-00)	0.44(-11)	1.9(-09)	4.3(-11)
1.0(+01)	0.32(-11)	1.4(-09)	3.1(-11)
1.2(+01)	0.23(-11)	1.1(-09)	2.4(-11)
1.5(+01)	0.18(-11)	7.7(-10)	1.8(-11)

Table 4.23. The rate coefficients $\bar{\alpha}^{DR}(cm^3/sec)$ and $\bar{\alpha}^{RE}(cm^3/sec)$ as functions of kT(Ry) for the transitions $d_1 \rightarrow d_2$, and $d_1 \rightarrow d_2 \rightarrow i_1, d_1$, respectively.

	$d_1 \rightarrow d_2$		
kT(Ry)	DR	i_1	d_1
1.0(-03)	1.4(-18)	6.2(-15)	2.1(-15)
2.0(-03)	7.0(-15)	3.0(-11)	1.2(-11)
4.0(-03)	3.4(-13)	1.5(-09)	8.4(-10)
6.0(-03)	1.0(-12)	4.4(-09)	3.2(-09)
8.0(-03)	1.6(-12)	7.0(-09)	5.7(-09)
1.0(-02)	1.9(-12)	8.7(-09)	7.7(-09)
3.0(-02)	4.3(-12)	1.1(-08)	1.3(-08)
5.0(-02)	1.1(-11)	9.2(-09)	1.2(-08)
8.0(-02)	2.0(-11)	7.3(-09)	1.0(-08)
1.0(-01)	2.2(-11)	6.2(-09)	8.7(-09)
3.0(-01)	1.4(-11)	2.1(-09)	3.0(-09)
5.0(-01)	8.4(-12)	1.1(-09)	1.6(-09)
8.0(-01)	4.8(-12)	5.9(-10)	8.6(-10)
1.0(-00)	3.6(-12)	4.4(-10)	6.3(-10)
3.0(-00)	7.8(-13)	9.0(-11)	1.3(-10)
5.0(-00)	3.7(-13)	4.2(-11)	6.1(-11)
8.0(-00)	1.9(-13)	2.1(-11)	3.1(-11)
1.0(+01)	1.3(-13)	1.5(-11)	2.2(-11)
1.2(+01)	1.0(-13)	1.2(-11)	1.7(-11)
1.5(+01)	7.3(-14)	8.3(-12)	1.2(-11)

Table 4.24. The rate coefficients $\bar{\alpha}^{DR}(cm^3/sec)$ and $\bar{\alpha}^{RE}(cm^3/sec)$ as functions of kT(Ry) for the transitions $i_1 \rightarrow d_3$, and $i_1 \rightarrow d_3 \rightarrow i_1, d_1, d_2$, respectively.

	$i_1 \rightarrow d_3$			
kT(Ry)	DR	i_1	d_1	d_2
1.0(-03)	6.9(-33)	2.4(-30)	1.4(-31)	5.1(-31)
2.0(-03)	2.5(-33)	8.3(-31)	4.9(-32)	1.8(-31)
4.0(-03)	8.7(-34)	2.9(-31)	1.7(-32)	6.3(-32)
6.0(-03)	4.7(-34)	1.6(-31)	9.4(-33)	3.5(-32)
8.0(-03)	3.4(-34)	7.7(-31)	6.1(-33)	2.2(-32)
1.0(-02)	1.6(-30)	3.4(-26)	4.4(-33)	1.6(-32)
3.0(-02)	2.9(-18)	6.2(-14)	1.2(-18)	1.7(-20)
5.0(-02)	6.5(-16)	1.4(-11)	8.5(-15)	1.1(-15)
8.0(-02)	1.3(-14)	2.6(-10)	1.0(-12)	4.9(-13)
1.0(-01)	4.2(-14)	6.6(-10)	4.9(-12)	3.5(-12)
3.0(-01)	3.5(-12)	4.9(-09)	1.7(-10)	3.8(-10)
5.0(-01)	6.9(-12)	5.3(-09)	2.3(-10)	6.4(-10)
8.0(-01)	7.8(-12)	4.3(-09)	2.1(-10)	6.6(-10)
1.0(-00)	7.3(-12)	3.7(-09)	1.9(-10)	6.0(-10)
3.0(-00)	2.9(-12)	1.1(-09)	6.3(-11)	2.2(-10)
5.0(-00)	1.6(-12)	5.8(-10)	3.3(-11)	1.2(-10)
8.0(-00)	8.5(-13)	3.0(-10)	1.7(-11)	6.3(-11)
1.0(+01)	6.2(-13)	2.2(-10)	1.3(-11)	4.6(-11)
1.2(+01)	4.8(-13)	1.7(-10)	9.8(-12)	3.6(-11)
1.5(+01)	3.5(-13)	1.2(-10)	7.1(-12)	2.6(-11)

Table 4.25. The rate coefficients $\bar{\alpha}^{DR}(cm^3/sec)$ and $\bar{\alpha}^{RE}(cm^3/sec)$ as functions of kT(Ry) for the transitions $d_1 \rightarrow d_3$, and $d_1 \rightarrow d_3 \rightarrow i_1, d_1, d_2$, respectively.

	$d_1 \rightarrow d_3$			
kT(Ry)	DR	i_1	d_1	d_2
1.0(-03)	2.0(-34)	6.9(-32)	2.3(-32)	2.3(-32)
2.0(-03)	5.2(-24)	5.8(-20)	3.6(-20)	8.2(-33)
4.0(-03)	6.0(-18)	6.7(-14)	4.2(-14)	1.7(-32)
6.0(-03)	4.8(-16)	5.4(-12)	3.4(-12)	9.3(-25)
8.0(-03)	3.8(-15)	4.3(-11)	2.7(-11)	7.0(-21)
1.0(-02)	1.2(-14)	1.4(-10)	8.6(-11)	1.4(-18)
3.0(-02)	1.4(-13)	1.6(-09)	9.2(-10)	1.3(-12)
5.0(-02)	1.7(-13)	2.0(-09)	1.0(-09)	1.7(-11)
8.0(-02)	2.4(-13)	1.8(-09)	8.5(-10)	6.5(-11)
1.0(-01)	3.4(-13)	1.7(-09)	7.4(-10)	9.6(-11)
3.0(-01)	8.7(-13)	7.3(-10)	2.8(-10)	1.5(-10)
5.0(-01)	7.3(-13)	4.2(-10)	1.5(-10)	1.1(-10)
8.0(-01)	5.0(-13)	2.4(-10)	8.4(-11)	6.7(-11)
1.0(-00)	4.0(-13)	1.8(-10)	6.3(-11)	5.2(-11)
3.0(-00)	1.0(-13)	3.9(-11)	1.3(-11)	1.3(-11)
5.0(-00)	5.2(-14)	1.9(-11)	6.4(-12)	6.1(-12)
8.0(-00)	2.6(-14)	9.4(-12)	3.2(-12)	3.1(-12)
1.0(+01)	1.9(-14)	6.8(-12)	2.3(-12)	2.2(-12)
1.2(+01)	1.5(-14)	5.2(-12)	1.7(-12)	1.7(-12)
1.5(+01)	1.1(-14)	3.7(-12)	1.3(-12)	1.2(-12)

Table 4.26. The rate coefficients $\bar{\alpha}^{DR}(cm^3/sec)$ and $\bar{\alpha}^{RE}(cm^3/sec)$ as functions of kT(Ry) for the transitions $d_2 \rightarrow d_3$, and $d_2 \rightarrow d_3 \rightarrow i_1, d_1, d_2$, respectively.

	$d_2 \rightarrow d_3$			
kT(Ry)	DR	i_1	d_1	d_2
1.0(-03)	4.7(-17)	4.3(-13)	1.8(-14)	2.7(-13)
2.0(-03)	6.2(-14)	4.7(-10)	1.9(-11)	3.1(-10)
4.0(-03)	1.9(-12)	1.0(-08)	4.0(-10)	6.8(-09)
6.0(-03)	5.0(-12)	2.3(-08)	9.1(-10)	1.6(-08)
8.0(-03)	7.2(-12)	3.0(-08)	1.3(-09)	2.1(-08)
1.0(-02)	8.5(-12)	3.4(-08)	1.5(-09)	2.4(-08)
3.0(-02)	8.5(-12)	2.4(-08)	1.5(-09)	1.9(-08)
5.0(-02)	1.4(-11)	1.8(-08)	1.3(-09)	1.5(-08)
8.0(-02)	2.7(-11)	1.3(-08)	1.0(-09)	1.1(-08)
1.0(-01)	3.3(-11)	1.1(-08)	9.1(-10)	9.6(-09)
3.0(-01)	3.1(-11)	3.9(-09)	3.5(-10)	3.5(-09)
5.0(-01)	2.0(-11)	2.1(-09)	1.9(-10)	1.9(-09)
8.0(-01)	1.2(-11)	1.1(-09)	1.0(-10)	1.0(-09)
1.0(-00)	9.2(-12)	8.4(-10)	7.7(-11)	7.7(-10)
3.0(-00)	2.1(-12)	1.7(-10)	1.6(-11)	1.6(-10)
5.0(-00)	1.0(-12)	8.3(-11)	7.7(-12)	7.6(-11)
8.0(-00)	5.1(-13)	4.1(-11)	3.8(-12)	3.8(-11)
1.0(+01)	3.7(-13)	3.0(-11)	2.8(-12)	2.7(-11)
1.2(+01)	2.8(-13)	2.3(-11)	2.1(-12)	2.1(-11)
1.5(+01)	2.0(-13)	1.6(-11)	1.5(-12)	1.5(-11)

Table 4.27. The rate coefficients $\bar{\alpha}^{DR}(cm^3/sec)$ and $\bar{\alpha}^{RE}(cm^3/sec)$ as functions of kT(Ry) for the transitions $i_1 \rightarrow d_4$, and $i_1 \rightarrow d_4 \rightarrow i_1, d_1, d_2, d_3$, respectively.

	$i_1 \rightarrow d_4$				
kT(Ry)	DR	i_1	d_1	d_2	d_3
1.0(-03)	9.5(-32)	2.5(-29)	1.4(-31)	5.1(-31)	1.9(-32)
2.0(-03)	3.4(-32)	8.7(-30)	4.9(-32)	1.8(-31)	6.8(-33)
4.0(-03)	1.2(-32)	3.1(-30)	1.7(-32)	6.4(-32)	2.4(-33)
6.0(-03)	6.5(-33)	1.7(-30)	9.5(-33)	3.5(-32)	1.3(-33)
8.0(-03)	4.2(-33)	1.1(-30)	6.1(-33)	2.3(-32)	8.5(-34)
1.0(-02)	5.4(-33)	3.1(-29)	4.4(-33)	1.6(-32)	6.1(-34)
3.0(-02)	1.7(-18)	2.3(-14)	1.7(-18)	1.3(-20)	2.0(-25)
5.0(-02)	1.2(-15)	1.8(-11)	6.8(-15)	8.3(-16)	4.5(-19)
8.0(-02)	5.1(-14)	6.8(-10)	6.9(-13)	3.7(-13)	1.3(-15)
1.0(-01)	2.1(-13)	2.2(-09)	3.2(-12)	2.8(-12)	1.7(-14)
3.0(-01)	3.6(-11)	3.4(-08)	1.3(-10)	3.3(-10)	7.6(-12)
5.0(-01)	8.0(-11)	4.3(-08)	2.0(-10)	5.9(-10)	1.7(-11)
8.0(-01)	9.5(-11)	3.8(-08)	1.9(-10)	6.3(-10)	2.0(-11)
1.0(-00)	9.2(-11)	3.4(-08)	1.7(-10)	5.8(-10)	1.9(-11)
3.0(-00)	3.9(-11)	1.1(-08)	6.2(-11)	2.2(-10)	7.9(-12)
5.0(-00)	2.1(-11)	5.9(-09)	3.3(-11)	1.2(-10)	4.3(-12)
8.0(-00)	1.1(-11)	3.1(-09)	1.7(-11)	6.3(-11)	2.3(-12)
1.0(+01)	8.4(-12)	2.3(-09)	1.3(-11)	4.6(-11)	1.7(-12)
1.2(+01)	6.5(-12)	1.7(-09)	9.8(-12)	3.6(-11)	1.3(-12)
1.5(+01)	4.8(-12)	1.3(-09)	7.1(-12)	2.6(-11)	9.7(-13)

Table 4.28. The rate coefficients $\bar{\alpha}^{DR}(cm^3/sec)$ and $\bar{\alpha}^{RE}(cm^3/sec)$ as functions of kT(Ry) for the transitions $d_1 \rightarrow d_4$, and $d_1 \rightarrow d_4 \rightarrow i_1, d_1, d_2, d_3$, respectively.

	$d_1 \rightarrow d_4$				
kT(Ry)	DR	i_1	d_1	d_2	d_3
1.0(-03)	6.3(-18)	1.0(-14)	3.3(-14)	3.9(-33)	7.0(-35)
2.0(-03)	1.8(-14)	3.0(-11)	9.5(-11)	1.4(-33)	2.5(-35)
4.0(-03)	5.7(-13)	9.5(-10)	3.0(-09)	5.9(-33)	8.8(-36)
6.0(-03)	1.4(-12)	2.3(-09)	7.4(-09)	1.9(-25)	4.8(-36)
8.0(-03)	1.9(-12)	3.2(-09)	1.0(-08)	1.0(-21)	3.1(-36)
1.0(-02)	2.2(-12)	3.6(-09)	1.1(-08)	1.6(-19)	6.2(-32)
3.0(-02)	1.4(-12)	2.3(-09)	7.3(-09)	1.1(-13)	2.0(-18)
5.0(-02)	1.0(-12)	1.6(-09)	4.5(-09)	1.7(-12)	7.6(-16)
8.0(-02)	1.0(-12)	1.2(-09)	2.8(-09)	7.7(-12)	1.7(-14)
1.0(-01)	1.2(-12)	1.1(-09)	2.3(-09)	1.2(-11)	4.2(-14)
3.0(-01)	3.4(-12)	5.7(-10)	8.0(-10)	2.2(-11)	2.4(-13)
5.0(-01)	3.1(-12)	3.6(-10)	4.6(-10)	1.6(-11)	2.2(-13)
8.0(-01)	2.3(-12)	2.2(-10)	2.6(-10)	1.1(-11)	1.6(-13)
1.0(-00)	1.8(-12)	1.7(-10)	2.0(-10)	8.4(-12)	1.3(-13)
3.0(-00)	5.0(-13)	3.8(-11)	4.4(-11)	2.1(-12)	3.6(-14)
5.0(-00)	2.5(-13)	1.9(-11)	2.1(-11)	1.0(-12)	1.8(-14)
8.0(-00)	1.3(-13)	9.4(-12)	1.1(-11)	5.2(-13)	9.2(-15)
1.0(+01)	9.3(-14)	6.8(-12)	7.6(-12)	3.7(-13)	6.7(-15)
1.2(+01)	7.1(-14)	5.2(-12)	5.8(-12)	2.9(-13)	5.1(-15)
1.5(+01)	5.1(-14)	3.7(-12)	4.1(-12)	2.1(-13)	3.7(-15)

Table 4.29. The rate coefficients $\bar{\alpha}^{DR}(cm^3/sec)$ and $\bar{\alpha}^{RE}(cm^3/sec)$ as functions of kT(Ry) for the transitions $d_2 \rightarrow d_4$, and $d_2 \rightarrow d_4 \rightarrow i_1, d_1, d_2, d_3$, respectively.

	$d_2 \rightarrow d_4$				
kT(Ry)	DR	i_1	d_1	d_2	d_3
1.0(-03)	2.1(-33)	2.6(-31)	4.5(-33)	7.9(-32)	1.1(-33)
2.0(-03)	2.0(-27)	5.0(-24)	1.9(-25)	2.7(-24)	3.8(-34)
4.0(-03)	3.5(-19)	8.6(-16)	3.2(-17)	4.7(-16)	1.4(-34)
6.0(-03)	1.5(-16)	3.8(-13)	1.4(-14)	2.0(-13)	5.6(-28)
8.0(-03)	2.8(-15)	7.0(-12)	2.5(-13)	3.7(-12)	5.4(-24)
1.0(-02)	1.5(-14)	3.8(-11)	1.4(-12)	2.0(-11)	1.8(-21)
3.0(-02)	8.5(-13)	2.2(-09)	6.0(-11)	9.0(-10)	3.3(-14)
5.0(-02)	2.2(-12)	4.0(-09)	9.5(-11)	1.4(-09)	7.6(-13)
8.0(-02)	6.0(-12)	4.8(-09)	1.0(-10)	1.6(-09)	3.5(-12)
1.0(-01)	8.7(-12)	4.9(-09)	1.0(-10)	1.6(-09)	5.2(-12)
3.0(-01)	1.4(-11)	2.7(-09)	4.9(-11)	8.2(-10)	7.5(-12)
5.0(-01)	9.8(-12)	1.6(-09)	2.8(-11)	4.8(-10)	5.2(-12)
8.0(-01)	6.2(-12)	9.1(-10)	1.6(-11)	2.7(-10)	3.2(-12)
1.0(-00)	4.8(-12)	6.8(-10)	1.2(-11)	2.1(-10)	2.5(-12)
3.0(-00)	1.2(-12)	1.5(-10)	2.6(-12)	4.5(-11)	5.9(-13)
5.0(-00)	5.6(-13)	7.2(-11)	1.2(-12)	2.1(-11)	2.8(-13)
8.0(-00)	2.8(-13)	3.6(-11)	6.2(-13)	1.1(-11)	1.4(-13)
1.0(+01)	2.1(-13)	2.6(-11)	4.4(-13)	7.7(-12)	1.0(-13)
1.2(+01)	1.6(-13)	2.0(-11)	3.4(-13)	5.9(-12)	7.9(-14)
1.5(+01)	1.1(-13)	1.4(-11)	2.4(-13)	4.2(-12)	5.7(-14)

Table 4.30. The rate coefficients $\overline{\alpha}^{DR}(cm^3/sec)$ and $\overline{\alpha}^{RE}(cm^3/sec)$ as functions of kT(Ry) for the transitions $d_3 \rightarrow d_4$, and $d_3 \rightarrow d_4 \rightarrow i_1, d_1, d_2, d_3$, respectively.

	$d_3 \rightarrow d_4$				
kT(Ry)	DR	i_1	d_1	d_2	d_3
1.0(-03)	3.2(-15)	4.4(-12)	2.0(-14)	8.4(-13)	2.6(-13)
2.0(-03)	3.4(-13)	4.6(-10)	2.0(-12)	7.4(-11)	2.5(-11)
4.0(-03)	3.2(-12)	3.6(-09)	1.7(-11)	4.7(-10)	2.1(-10)
6.0(-03)	6.9(-12)	6.4(-09)	3.4(-11)	7.6(-10)	4.1(-10)
8.0(-03)	1.0(-11)	8.1(-09)	4.6(-11)	9.2(-10)	5.6(-10)
1.0(-02)	1.5(-11)	9.2(-09)	5.4(-11)	1.0(-09)	6.6(-10)
3.0(-02)	7.3(-11)	8.8(-09)	5.7(-11)	8.9(-10)	7.3(-10)
5.0(-02)	8.6(-11)	6.4(-09)	4.3(-11)	6.4(-10)	5.4(-10)
8.0(-02)	7.3(-11)	4.2(-09)	2.8(-11)	4.1(-10)	3.6(-10)
1.0(-01)	6.2(-11)	3.3(-09)	2.2(-11)	3.2(-10)	2.8(-10)
3.0(-01)	2.0(-11)	8.4(-10)	5.7(-12)	8.1(-11)	7.3(-11)
5.0(-01)	1.0(-11)	4.1(-10)	2.8(-12)	4.0(-11)	3.6(-11)
8.0(-01)	5.3(-12)	2.1(-10)	1.4(-12)	2.0(-11)	1.8(-11)
1.0(-00)	3.8(-12)	1.5(-10)	1.0(-12)	1.5(-11)	1.3(-11)
3.0(-00)	7.8(-13)	3.0(-11)	2.0(-13)	2.9(-12)	2.6(-12)
5.0(-00)	3.6(-13)	1.4(-11)	9.5(-14)	1.3(-12)	1.2(-12)
8.0(-00)	1.8(-13)	7.0(-12)	4.7(-14)	6.7(-13)	6.1(-13)
1.0(+01)	1.3(-13)	5.0(-12)	3.4(-14)	4.8(-13)	4.4(-13)
1.2(+01)	9.9(-14)	3.8(-12)	2.6(-14)	3.6(-13)	3.3(-13)
1.5(+01)	7.1(-14)	2.7(-12)	1.8(-14)	2.6(-13)	2.4(-13)

APPENDIX A

Scaling Properties of A_a, A_r, $\omega(d)$, and α^{DR}

Z-Scaling:

$\underline{\Delta n \neq 0}$

Aa (ab→tc) contains one cotinuum orbital c and three bound orbitals a, b, and t. The Z-dependence appears in the normalization factors, as

$$U_a, U_b, U_t \sim Z^{3/2}$$

$$U_c \rightarrow \left(\frac{2}{\pi k_c}\right)^{1/2} \frac{1}{r} \sin\left(k_c r - \frac{l_c \pi}{2} + \frac{Z}{k_c}\log_c(2k_c r) + \sigma_{lc}\right)$$

$$\sim Z^{1/2}$$

where $k_c \sim Z$ and $r \sim Z^{-1}$

thus we have

$$A_a \sim |\langle a\, b \left| \frac{1}{r_{12}} \right| t\, c \rangle|^2 \sim Z$$

On the other hand, A_r(b→f) involves two bound orbials, thus we have,

$$A_r \sim Z^4$$

The dependence of $\omega(d)$ on Z is more complicated,

$$\omega(d) = \Gamma_r(d)/\Gamma(d) \quad , \quad \Gamma(d) = \Gamma_r(d) + \Gamma_a(d)$$

$$\omega(d) \sim Z^0 \quad \text{for} \quad \Gamma_r >> \Gamma_a \quad \text{and} \quad \omega(d) \approx 1$$

$$\omega(d) \sim Z^4 \quad \text{for} \quad \Gamma_r << \Gamma_a \quad \text{and} \quad \omega(d) << 1$$

Thus

$$\alpha^{DR} \sim Z^{-3} \quad \text{for} \quad \omega(d) \approx 1$$

$$\alpha^{DR} \sim Z \quad \text{for} \quad \omega(d) << 1$$

$$\bar{\sigma}^{DR} \sim Z^{-4} \quad \text{for} \quad \omega(d) \approx 1$$

$$\bar{\sigma}^{DR} \sim Z^0 \quad \text{for} \quad \omega(d) << 1$$

APPENDIX B

Example of Calculation

$$\bar{\sigma}^{DR} = \frac{4\pi(Ry)}{e_c(Ry)}\ \tau_0\, V_a(i\rightarrow d)\ \omega(d)\ \frac{1}{\Delta e_c}\ (\pi\, a_0^2)$$

$\tau_0 = 2.42 \times 10^{-17}$ sec

$a_0 = 5.29 \times 10\text{-}9$ cm , $\pi\, a_0^2 = 8.79 \times 10^{-17}$ cm^2

$V_a = (g_d/2g_i)\ A_a$

$\omega(d) = A_r/(\Gamma_a + \Gamma_r)$

The reaction we have is,

$$(3s\ 3p^2)^4P + e_c \rightarrow (3s^2\ 3p)^2P\ ,\ k_c\ \ell_c$$

$\Delta e_c = 0.01$ Ry , $e_c = 0.193$ Ry

$A_r = 3.31 \times 10^8$ sec^{-1} , $A_a = 1.38 \times 10^{14}$ sec^{-1}

$\ell = 1$, $s = 1$

$g_d = (2s + 1)(2l + 1) = 9$

$g_i(^2P) = (2s + 1)(2l + 1) = 6$

$V_a = 1.035 \times 10^{14}$ sec^{-1}

$\bar{\sigma}^{DR} = 3.44 \times 10^{-21}$ cm^2

$$\overline{\sigma}^{DR} = (4.06 \times 10^{-9}) \frac{kT}{(Ry)^{3/2}} \frac{e^{e_c/kT}}{e_c \Delta e_c} \overline{\alpha}^{DR}$$

kT is arbitrary, take 1.5 Ry

$\overline{\alpha}^{DR} = 7.85 \times 10^{-16}$ cm^3/sec

APPENDIX C

High Rydberg States Energies (Ry)

n ℓ	^4P	^2D	^2S	^2P
4 s	-0.573	-0.367	-0.095	-0.005
5 s	0.010	0.216	0.488	0.578
6 s	0.254	0.460	0.732	0.822
7 s	0.381	0.587	0.859	0.949
8 s	0.456	0.662	0.934	1.024
9 s	0.503	0.709	0.981	1.071
10 s	0.524	0.730	1.002	1.092
11 s	0.540	0.746	1.018	1.108
12 s	0.552	0.758	1.030	1.120
4 p	-0.344	-0.138	0.134	0.224
5 p	0.102	0.308	0.580	0.670
6 p	0.300	0.506	0.778	0.868
7 p	0.408	0.613	0.886	0.976
8 p	0.472	0.678	0.950	1.040
9 p	0.514	0.720	0.992	1.082
10 p	0.535	0.741	1.013	1.103
11 p	0.551	0.757	1.029	1.119
12 p	0.563	0.769	1.041	1.131
3 d	-0.714	-0.508	-0.236	-0.146
4 d	-0.032	0.174	0.446	0.536
5 d	0.234	0.440	0.712	0.802
6 d	0.370	0.576	0.848	0.938
7 d	0.449	0.655	0.927	1.017
8 d	0.498	0.704	0.976	1.066
9 d	0.532	0.738	1.010	1.100
10 d	0.553	0.759	1.031	1.121
11 d	0.569	0.775	1.047	1.137
12 d	0.581	0.787	1.059	1.149

n ℓ	^4P	^2D	^2S	^2P
4 f	0.068	0.274	0.546	0.636
5 f	0.282	0.488	0.760	0.850
6 f	0.396	0.602	0.874	0.964
7 f	0.465	0.671	0.943	1.033
8 f	0.509	0.715	0.987	1.077
9 f	0.539	0.745	1.017	1.107
10 f	0.561	0.766	1.038	1.128
11 f	0.576	0.782	1.054	1.144
12 f	0.588	0.794	1.066	1.156
5 g	0.290	0.496	0.768	0.858
6 g	0.400	0.606	0.878	0.968
7 g	0.467	0.673	0.945	1.035
8 g	0.511	0.717	0.989	1.079
9 g	0.541	0.747	1.019	1.109
10 g	0.562	0.768	1.040	1.130
11 g	0.577	0.783	1.055	1.145
12 g	0.589	0.795	1.067	1.157
6 h	0.402	0.608	0.880	0.970
7 h	0.468	0.674	0.946	1.036
8 h	0.512	0.717	0.989	1.079
9 h	0.541	0.747	1.019	1.109
10 h	0.562	0.768	1.040	1.130
11 h	0.578	0.784	1.056	1.146
12 h	0.590	0.796	1.068	1.158

REFERENCES

1. H. S. W. Massey and D. R. Bates, Rep. Prog. Phys. 9, 62 (1942).
2. A. Burgess, Astrophys. J. 139, 776 (1964).
3. Y. Hahn, in Advances in Atomic and Molecular Physics, editors D.R. Bates and B. Bederson, 21, 123 (1985).
4. G. Omar, Ph. D. dissertation, University of Connecticut (1987).
5. I. Nasser, Ph. D. dissertation, University of Connecticut (1985).
6. D. J. McLaughlin, Ph. D. dissertation, University of Connecticut. (1983).
7. H. H. Ramadan, Ph. D. dissertation, University of Connecticut (1989).
8. See any book in atomic physics, for example M. Weissbluth, Atoms and Molecules .(Academic Press) 1978.
9. G. Omar and Y. Hahn, Phys. Rev. A, 37, 1983 (1988).
10. Y. Hahn. and K. LaGattuta, Phys. Rep. 166, 195 (1988).
11. I. Nasser, AJSE, 16, 85 (1991).
12. P. F. Dittner, S. Datz, R. Hippler, H. F. Krause, P.D. Miller, P. L. Pepmiller, C. M. Fou, Y. Hahn and I. Nasser, Phys. Rev. A, 38, 2762 (1988).
13. S. Bashkin and J. O. Stoner, Jr., Atomic Energy Levels and Grotrian Diagrams (North-Holland, Amsterdam,

1977).

14. Y. Hahn, Adv. At. Mol. Phys. **21**, 123 (1985).
15. Y. Hahn. and K. LaGattuta, Phys. Rep. **166**, 195 (1988).
16. D. E. Shemansky, J. Geophys. Res. **92**, 6141 (1988).
17. N. R. Badnell, Astrophys. J. **379**, 356 (1991).
18. R. D. Cowan, The Theory of Atomic Structrue and Spectra (University of California Press, Berkeley, 1981).
19. I. Nasser and Y. Hahn, Phys. Rev. A. **44**, 6133 (1991).
20. P. F. Dittner, S. Datz, R. Hippler, H. F. Krause, P. D. Miller, P. L. Pepmiller, C. M. Fou, Y. Hahn and I. Nasser, Phys. Rev. A. **38**, 2762 (1988).
21. N. R. Badnell, M. S. Pindzola, L. H. Anderson, J. Bolko, and H. T. Schmidt, J. Phys. B. : At. Mol. Opt. Phys. **24**, 4441, (1991).
22. V. L. Jacobs, J. Davis, J. E. Rogerson, and M. Blaha, Astrophys. J. **230**, 627 (1979).
23. I. Nasser and Y. Hahn, J. Phys. B. : At. Mol. Opt. Phys. **25**, 521, (1992)